

# 2

## Satellite systems for studies of atmospheric ozone

It is now slightly over 50 years since the era of satellite remote sensing began on October 4, 1957, when the former Soviet Union launched Sputnik 1, the world's first artificial satellite (a 55 cm diameter sphere that weighed 83 kg with four antennae attached to it) (Figure 1.1). In the intervening years, satellites have revolutionized the Earth sciences, including the study of trace gases, in general, and ozone, in particular. With the passage of time, satellite-flown instruments became more complicated, while larger satellites carrying more and more instruments were launched. One of the largest of these was ENVISAT (ENVironmental SATellite) which was launched on March 1, 2002 by the European Space Agency (ESA), with a mass of 8,211 kg and dimensions in orbit of 26 m  $\times$  10 m  $\times$  5 m. It was a Sun-synchronous satellite flown at an altitude of 800 km, with an inclination of 98° and an orbital period of 101 min. It carried instruments for monitoring the Earth's land, atmosphere, oceans, and ice caps (Figure 1.1) (<http://envisat.esa.int/>) and three of these were particularly relevant to atmospheric ozone (see Section 2.3.6). It successfully reached its nominal 5-year mission lifetime, having orbited the Earth more than 26,000 times. Figure 1.1c shows Sputnik on the same scale as ENVISAT in Figure 1.1b.

Recently, we have been seeing a trend to move away from large multifunctional Earth-observing satellites, like ENVISAT, to small satellites dedicated to one particular observational task. The advantages of this include simple and speedy design and manufacture, many more launch opportunities, low cost, non-competition between the requirements of different instruments, risk reduction, etc. Small satellites also provide opportunities for developing countries to become involved in technology transfer and the development of indigenous space-related capabilities. Thus we foresee a role for both large and small Earth-observing satellites in the future (Cracknell and Varotsos, 2007a).

However, before considering satellite remote sensing of atmospheric ozone we should also consider the use of aircraft. There have been a few studies of the atmo-

sphere using instruments flown on aircraft to study ozone and related chemicals directly, most notably in the early study of the Antarctic ozone hole, using a modified U-2 spy plane called ER-2 (see Section 5.6). However, many of the satellite-flown instruments we discuss in this chapter have similar counterparts flown on aircraft as well. There have usually been two reasons for this. The first is for calibrating and evaluating prototypes of the instruments before flying them in space. The second is for simultaneous flying of similar (nominally identical) instruments in aircraft and in space for validation of the spaceborne instrument. Some instances of airborne versions of instruments will be given in later sections in this chapter. However, there is another rather new aspect of airborne remote sensing which we should mention.

Just as remote-sensing satellites for environmental studies can be regarded as a spin-off development from military spy satellites, so we are now seeing a similar spin-off from unmanned military aircraft in a new mission called Global Hawk Pacific, or GloPac, and one or two other unmanned aircraft NASA projects. NASA has staged environmental (manned) research flights from aircraft previously, but none has had the reach and duration of Global Hawk, a high-altitude, unmanned aircraft. The aircraft, which is distinguished by its bulbous nose and 35.4 m wingspan, can travel about 18,500 km in up to 31 hours, carrying almost 1 t of instrument payload. By contrast, NASA's manned research aircraft, the ER-2, can fly for only eight hours. Furthermore, researchers do not have access to their data until after the ER-2 aircraft lands (<http://gsfctechnology.gsfc.nasa.gov/GlobalHawk.htm>).

NASA has taken over two Global Hawk unmanned aircraft that were originally built by Northrop Grumman for the U.S. Defense Advanced Research Projects Agency. The first two test flights were made on April 6 and April 13, 2010. These two flights were part of the five-flight GloPac mission to study the atmosphere over the Pacific and Arctic Oceans—NASA's first Earth science project to make use of unmanned aircraft, two of which were transferred from the U.S. Air Force to be based at NASA Dryden Flight Research Center on Edwards Air Force Base in California.

The Global Hawk aircraft used in the GloPac mission carried a suite of 12 instruments—provided by scientists from the Goddard Space Flight Center, the Jet Propulsion Laboratory, the National Oceanic and Atmospheric Administration (NOAA), Denver University, and the Ames Research Center. The first operational flights of the Global Hawk for GloPac were conducted in support of the Aura Validation Experiment (AVE). This was planned to encompass the entire offshore Pacific region with four to five 30 hour flights. Aura is one of the A-Train satellites (Figure 2.1) supported by the NASA Earth Observation System (<http://www.espo.nasa.gov/glopac/>). The NASA A-Train is a convoy of Earth-observing spacecraft following one another in polar orbit. Initially the A-Train comprised four satellites—Aqua, CloudSat, Cloud-Aerosol Lidar and Infrared Pathfinder Satellite Observations (CALIPSO) and Aura—which pass in sequence across the equator each day at around 1:30 PM local time each afternoon and carry between them 15 separate scientific instruments. From time to time further satellites are added to the A-Train (e.g., PARASOL and OCO satellites). Having several individual satellites in

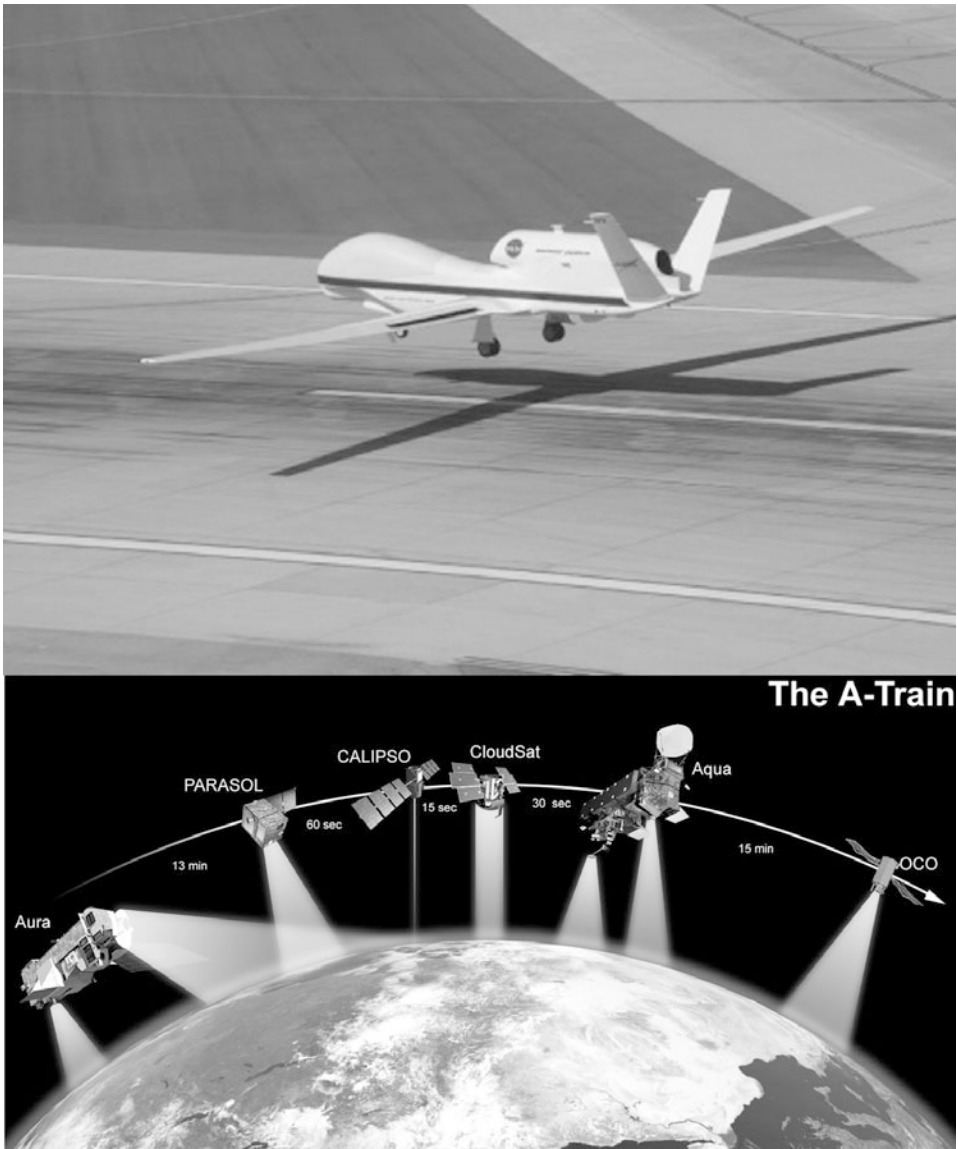


**Figure 2.1.** A NASA Global Hawk lands at Dryden (top) and the A-Train (bottom) (*source: NASA*).

the A-Train avoids some of the engineering problems that would arise if one attempted the impossible by assembling 15 or more instruments on one large spacecraft like ENVISAT. The Global Hawk flights were designed to address various science objectives:

1. validation and scientific collaboration with NASA Earth-monitoring satellite missions, principally the Aura satellite;
2. observations of stratospheric trace gases in the upper troposphere and lower stratosphere from the mid-latitudes to the tropics;
3. sampling of polar stratospheric air and the break-up fragments of the air that move into the mid-latitudes;
4. measurements of dust, smoke, and pollution that cross the Pacific from Asia and Siberia;
5. measurements of streamers of moist air from the central tropical Pacific that move onto the West Coast of the United States (atmospheric rivers).

## 2.1 SATELLITE REMOTE SOUNDING OF TOC

We now turn to the satellite remote sensing of ozone. A number of instruments measure ozone vertical profiles and TOC from space by measuring backscattered UV solar radiation. The spectral distribution of backscattered radiation to space by the Earth's atmosphere depends on the presence of gases with selective absorption bands and molecular (Rayleigh) as well as aerosol scattering. The instruments can use spectrometers or filters for various spectral channels and they can observe in the nadir direction—as for solar-backscattered UV) or through scanning cross-tracks (as with total ozone-mapping spectrometry (Grant, 1989). These instruments operate best above 15–20 km (where there is strong absorption by ozone in the Hartley band).

During the second half of the 1960s several attempts at satellite remote sounding of ozone and other minor gas components from Soviet manned spacecraft were first made, using a hand-held spectrograph, and a complex of solar spectrometers functioning in a regime of occultation geometry (Kondratyev, 1972; Kondratyev *et al.*, 1996).

Since 1970, appropriate instrumentation launched on board various satellites (e.g., Nimbus-4), has provided values of the global distribution of TOC with very good spatiotemporal coverage. In the early days, TOC monitoring was carried out with NOAA's TOVS and its predecessors, with NASA's and METEOR's TOMS (Total Ozone Monitoring Spectrometer) and with the SBUV (Solar Backscatter UV), all instruments that were first flown on satellites in 1978. These measurements continued with SBUV/2 instruments on board the NOAA-9, -11, -14, -16, and -17 satellites, and TOMS instruments on the Russian Meteor-3, Earth Probe, and Japanese ADEOS satellites until the year 2003 (when instrument degradation was observed). The European Space Agency's GOME on the ERS-2 satellite, also performing BUV measurements, complemented the U.S. efforts. In addition, the Shuttle SBUV (SSBUV) experiment (conducting eight missions between October 1989 and January 1996) provided regular checks on the calibration of individual satellite instruments. Hilsenrath *et al.* (1997) summarized the contributions of the SSBUV (eight Space Shuttle missions from October 1989 to January 1996) in support of the U.S. long-term ozone-monitoring program (mainly from the viewpoint of validation

of satellite observations). A significant decrease in Northern Hemisphere TOC from the winter of 1992 to the following winter was observed. However, the TOMS time series was interrupted during May 1993–July 1996 when TOMS/EP (Total Ozone Monitoring Spectrometer/Earth Probe Satellite) was launched. This gap was filled by continuous SBUV observations on various NOAA satellite missions and some GOME ozone observations since July 1995 aboard ERS-2, the first European satellite instrument measuring total ozone from the UV–VIS. An important source of minor gas components data is the TERRA satellite launched in December 1999. An instrumental problem in 2003 reduced the global coverage of GOME. Follow-up European satellite instruments are SCIAMACHY launched in 2002 on the ENVISAT platform of the European Space Agency (ESA) and OMI, a Dutch–Finnish instrument on the NASA EOS–Aura platform launched in 2004 and then later on the first European polar-orbiting meteorological satellite MetOp (Kaye, 1997). The first MetOp satellite (MetOp-A) was launched on October 19, 2006 and was declared fully operational in mid-May 2007. In addition, an interesting aspect of the OMI is also its synergy with the ENVISAT and GOME missions (Dobber *et al.*, 2006). The UV–VIS spectrometer GOME-2 was launched in 2006 on the first of a series of three operational EUMETSAT MetOp missions, which should allow continuous ozone monitoring until about 2020.

Multiple intercomparisons with ground-based instruments (e.g., Brewer, Dobson, and filter instruments) improved data-retrieval algorithms and therefore satellite observations of TOC became compatible with ground-based ones (Fioletov *et al.*, 2008; McPeters and Labow, 1996; see Chapter 3).

In the U.S. ozone research plans include both a total ozone mapper and an ozone-profiling instrument for the National Polar-orbiting Operational Environmental Satellite System (NPOESS; see Section 2.3.7).

A brief description of the satellite instrumentation providing TOC observations is given in Sections 2.3.1, 2.3.2, and 2.3.6, grouped by type of measurement (direct absorption, indirect absorption, and emission). It should be noted that several instruments provide not only TOC, but also OVP measurements.

## 2.2 DIRECT ABSORPTION MEASURING INSTRUMENTS

In this section brief information is given for a few instruments that are used to measure TOC by directly measuring the absorption features of ozone, either within a path defined by the instrument or by using an extraterrestrial source such as the Sun.

### 2.2.1 TIROS Operational Vertical Sounder (TOVS); GOES

The Television InfraRed Observational Satellite (TIROS)-N and its successors in the NOAA series of polar-orbiting meteorological satellites carried the TIROS Operational Vertical Sounder (TOVS) on board; later satellites in the program carried an

Advanced TOVS or ATOVS with more spectral channels. The TOVS is a set of three instruments—the High Resolution Infrared Sounder (HIRS/2), the Stratospheric Sounding Unit (SSU), and the Microwave Sounding Unit (MSU)—providing 27 spectral channels which are all, except one, in the infrared and microwave region of the spectrum with one panchromatic channel. The three instruments are used together to provide the vertical profiles of pressure, temperature, and humidity in the atmosphere. On later spacecraft in the NOAA series of polar orbiters there was the improved ATOVS (Advanced TOVS) with improved versions of the HIRS (HIRS/4) and the MSU (the AMSU, Advanced MSU) (Kramer, 2002).

HIRS has 19 infrared channels (3.8–15  $\mu\text{m}$ ) and 1 visible channel. The swath width is 2,160 km with 10 km resolution at nadir. The HIRS/4 instrument provides multispectral data from one visible channel (0.69  $\mu\text{m}$ ), 7 shortwave channels (3.7 to 4.6  $\mu\text{m}$ ) and 12 longwave channels (6.7 to 15  $\mu\text{m}$ ) using a single telescope and a rotating filter wheel containing 20 individual spectral filters. A rotating scan mirror provides cross-track scanning of 56 steps in increments of 1.8 degrees. The mirror steps rapidly (<35 ms), then holds at each position while optical radiation, passing through the 20 spectral filters, is sampled. This action takes place every 0.1 s. The instantaneous field of view for each channel is approximately  $0.7^\circ$  which, from a spacecraft altitude of 837 km, encompasses a circular area of 10 km at nadir on the Earth. Three detectors are used to sense optical radiation. A silicon photodiode, at nominal instrument temperature ( $15^\circ\text{C}$ ), detects the visible radiation. An Indium Antimonide detector and Mercury Cadmium Telluride detector (mounted on a passive radiator and operating at 95 K) sense the shortwave and longwave IR radiation, respectively. The shortwave and visible optical paths have a common field stop, while the longwave path has an identical but separate field stop. The size and registration of the optical fields of view in all channels is determined by these stops. IR calibration of the HIRS/4 is provided by programmed views of two radiometric targets: the warm target mounted on the instrument baseplate and a view of deep space. Data from these views provides sensitivity calibrations for each channel at 256 s intervals if commanded. It uses  $\text{CO}_2$  absorption bands for temperature sounding ( $\text{CO}_2$  is uniformly mixed in the atmosphere). In addition, it measures water vapor, ozone,  $\text{N}_2\text{O}$ , and cloud and surface temperatures.

Channel 9 of the HIRS, at a wavelength of 9.7  $\mu\text{m}$ , is particularly well suited for monitoring stratospheric ozone concentration; this is a (general) window channel, except for absorption by ozone. Thus, the radiation received by the HIRS instrument was emitted from the Earth's surface and not from various levels in the Earth's atmosphere, but it is attenuated by the ozone in the atmosphere. The less ozone, the greater the amount of radiation reaching the satellite. A 3 DU drop in lower-stratospheric ozone produces a measurable (circa  $0.2^\circ\text{C}$ ) increase in the brightness temperature in this channel. It appears that, strictly speaking, what is measured is lower-stratospheric ozone and a correction has to be applied to obtain total column ozone (TOC). Images are now regularly produced from TOVS data giving hemispherical daily values of total ozone. This means that there is now a long time series of such data available. TOVS data have been used to determine atmospheric ozone concentration from 1978 to the present (Neuendorffer, 1996; Kondratyev, 1997,



1998b) and the standard deviation is approximately 7%. Nowadays, TOVS data are also used when the more reliable TOMS data are not available (<http://www.theozonehole.com/2010oct.htm>). Since TOVS ozone data are only sensitive to variations in the lower stratosphere, long-term TOVS total ozone trends are, at best, only indicative of lower-stratospheric ozone trends. An advantage of TOVS over other systems that use solar UV radiation is that TOVS data are available at nighttime and in the polar regions in winter. The drawbacks are that when the Earth's surface is too cold (e.g., in the high Antarctic Plateau), too hot (e.g., the Sahara desert), or too obscured (e.g., by heavy tropical cirrus clouds) the accuracy of this method declines.

Li *et al.* (2001) discussed the potential for using Geostationary Operational Environmental Satellite (GOES) Sounder radiance measurements to monitor total atmospheric ozone with a statistical regression using GOES Sounder spectral band 1–15 radiances. The advantage is the high temporal frequency of the availability of the data. Hourly GOES ozone products have been generated since May 1998. GOES ozone estimates were compared with TOMS TOC data and ozone measurements from ground-based Dobson spectrometer ozone observations. The results showed that the percentage root-mean-square (rms) difference between instantaneous TOMS and GOES ozone estimates ranged from 4% to 7%. Also, daily comparisons for 1998 between GOES ozone values and ground-based observations at Bismarck (North Dakota), Wallops Island (Virginia), and Nashville (Tennessee) show that the rms difference is approximately 21 DU.

### 2.2.2 Laser Heterodyne Spectrometer (LHS)/Tunable Diode LHS (TDLHS)

This spectrometer measures TOC by performing observations of the ozone profiles in the 0.9  $\mu\text{m}$  region in the infrared. A laser is used as a local oscillator to direct a narrow bandwidth beam onto a detector or photomixer. Usually a  $\text{CO}_2$  laser is used as the local oscillator, but occasionally a tunable diode laser is employed. The Sun or the Moon acts as the source of radiation beyond the atmosphere. Radiation is selectively absorbed by ozone or other molecular species in the atmosphere and is detected by the spectrometer. A TDLHS system was used as a ground-based station instrument at the University of Denver to determine TOC (McElroy *et al.*, 1991). A  $\text{CO}_2$  and TDLHS can also be used to measure the OVP. Such measurements can be made with a vertical resolution of 4 km, which is limited by the rate of change in the spectral weighting functions with altitude or with lower resolution, if an insufficient number of channels are used. The accuracy of the measurements is approximately 5–10% for column content and 10–30% for profile measurements. The precision is approximately 2%. The advantages of the LHS over other techniques are its ultra-high spectral resolution, high spatial resolution, high quantum detection efficiency, and very good signal-to-noise ratio. The high resolution makes the system very selective as interference problems due to overlapping lines or bands are minimized (Fogal *et al.*, 1989).

**Table 2.1.** Instruments on board the PRIRODA module of the *Mir* Space Station.

<i>Instrument</i>	<i>Spectral range</i>	<i>Channels/ Bandwidth</i>	<i>Swath</i>	<i>Spatial resolution</i>	<i>Remarks</i>
MSU-SK	0.5–12.5 $\mu\text{m}$	5/100 nm	350 km	120 $\times$ 300 m	Conical scanner
MSU-E	0.5–0.9 $\mu\text{m}$	3/100 nm	45 km	25 m	Pushbroom scanner
MOS-A	757–767 nm	4/1.4 nm	80 km	2.7 km	Imaging spectrometer
MOS-B	408–1,010 nm	13/10 nm	80 km	650 m	Imaging spectrometer
ALISA	532 nm	—	3'	150 m (vertical)	LIDAR Pulse Power (40 mJ)
TV camera	400–750 nm	—	15°	300 m	Color
MOMS-2P	400–750 nm	4 + 3/80 nm	44/88 km	5/16 m	Stereo/MS
OZON-MIR	0.26–1 $\mu\text{m}$	4	2' $\times$ 25'	—	Occultation

### 2.2.3 OZON-MIR

The PRIRODA module of the *Mir* Space Station was launched in mid-1996. This module has two instruments on board, known as OZON-MIR and ISTOK-1. These instruments use the occultation technique to measure the concentrations of a number of trace gases and aerosols. ISTOK-1 also has a limb emission mode, although retrieval studies suggest that the errors in this mode are considerably larger than in the occultation mode (WMO, 1999). The instruments and their specifications are given in [Table 2.1](#).

## 2.3 INDIRECT ABSORPTION MEASURING INSTRUMENTS

For a decade or two the principal instruments for studying TOC from satellites were the TOMS (Total Ozone Monitoring Spectrometer) and the SBUV (Solar Backscatter UV radiometer), although the SBUV was also capable of profiling (i.e., studying the OVP). TOMS is a scanning instrument that enables total ozone, TOC, to be determined. The SBUV is a nadir-pointing profiling instrument which enables both TOC and the vertical profile, OVP, to be determined. We consider the TOMS first.

### 2.3.1 Total Ozone Mapping Spectrometer (TOMS)

At about the same time that the first TOVS was flown, the Nimbus-7 satellite was launched and this carried, among other instruments, the first Total Ozone Mapping



Spectrometer (TOMS). A schematic diagram of the Nimbus-7 TOMS is shown in [Figure 2.2](#).

The TOMS uses a similar principle to that of the Dobson spectrophotometer: it utilizes the wavelength dependence of the Earth's ultraviolet albedo in the Huggins band of the ozone absorption spectrum. The TOMS uses a single monochromator and scans across the sub-orbital track, sampling radiation backscattered from the underlying surface and atmosphere. It uses an infrared cloud cover photometer to avoid problems from clouds. It has six UV wavelength bands from 312.5 to 380 nm (see [Table 2.2](#)), and TOC is inferred by utilizing the wavelength dependence of the Earth's ultraviolet albedo in the Huggins band of the ozone absorption spectrum. The first four wavelength regions are used in pairs to provide three estimates of ozone concentration by the differential absorption method, while the other two (free of ozone absorption) are used to determine the effective background albedo. The Temperature Humidity Infrared Radiometer (THIR) on board the satellite is used to determine cloud locations and heights. Precision is quoted as 2% or better (with a small drift in diffuser plate reflectance of 0.4% per year). The TOMS instrument flown on the Nimbus-7 satellite and its successors have been used to measure the global distribution of ozone. This instrument was followed by the TOMS flown on the Meteor-3 satellite. The time that had elapsed since the Nimbus-7 TOMS was designed and built enabled some improvements to be incorporated in the Meteor-3 TOMS.

The basic differences between the Meteor-3 TOMS (engineering model) and the Nimbus-7 TOMS instrument were the following:

- An Interface Adapter Model (IAM) was added to make the TOMS instrument compatible with Meteor-3, which was launched on August 15, 1991 in an orbit with an 82.5° inclination. The orbit precessed relative to the Earth–Sun line with a period of 212 days, unlike Nimbus-7 which had a Sun-synchronous orbit. For two periods within this cycle the instrument was close to the terminator and this made ozone retrieval difficult.
- Replacement of the single diffuser with a three-diffuser carousel allowed calibration by comparison of diffusers with different rates of exposure.
- The higher altitude of Meteor-3/TOMS (1,200 km compared to 996 km for Nimbus-7/TOMS) meant greater overlap between successive orbits for the Meteor-3/TOMS than for Nimbus-7/TOMS.
- The Meteor-3 instrument was further improved when the diffraction grating was replaced, the mirrors resurfaced, flight-qualified electronics added, and a solid-state data recorder replaced the tape recorder, which had been used for Nimbus-7 and so almost no data were lost during the 3-year mission.

To obtain daily high-resolution global maps of atmospheric ozone, Meteor-3/TOMS measured solar irradiance and the radiance backscattered by the Earth's atmosphere in six (1 nm) selected wavelength bands in the ultraviolet. The experiment used a single monochromator and scanning mirror to sample backscattered

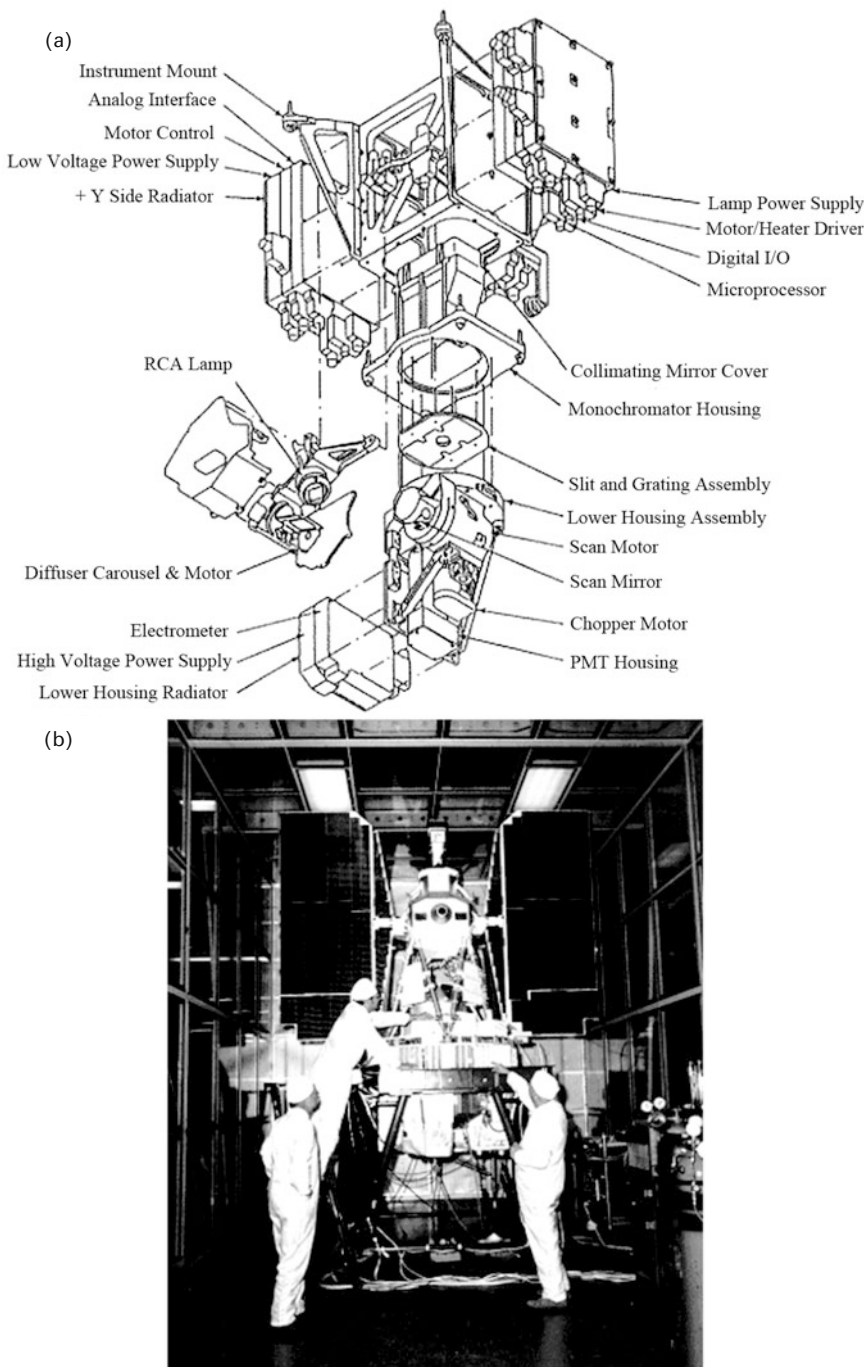


**Figure 2.2.** (a) TOMS optical diagram and (b) the Nimbus-7 spacecraft which carried the first TOMS instrument, before its launch in 1978 (NASA).

**Table 2.2.** TOMS main characteristics (McPeters and Labow, 1996).

Spectral bands	6
Wavelengths	312.3, 317.4, 331.1, 339.7, 360, 380 nm
Bandwidth	1.0 nm
Total ozone accuracy	<2%
Ozone trend accuracy (goal)	1% per decade
Sulphur dioxide accuracy	±25%
Scan time	6.3 s
Data rate	approx. 700 bps
Mass	<33 kg
Power	<20 W

SUVR at 35 sample points at 3° intervals. It scanned the Earth in 3° steps to 51° on each side of the sub-satellite point in a direction perpendicular to the orbital plane.

In normal operation, the scanner measured 35 scenes, one for each scanner view angle stepping from right to left. It then quickly returned to the first position, not performing measurements on the retrace. Eight seconds after the start of the previous scan, another scan would begin. Observations used for ozone retrieval were made during the sunlit portions of the orbit.

The measurements made using the TOMS on board the Meteor-3 satellite began on August 22, 1991 and ended on December 28, 1994. This system provided daily global coverage of the Earth's TOC by measuring backscattered Earth radiance. These data were archived at the Goddard Space Flight Center (GSFC), Distributed Active Archive Center (DAAC) and have been processed independently by the Central Aerological Observatory (CAO) of the Russian State Committee on Hydro-meteorology. There was a one-and-a-half-year overlap between Nimbus-7 and Meteor-3 permitted an intercalibration that allows the data from the two satellites to be used to form a continuous 16-year dataset, which can be used to study ozone trends from November 1978 to December 1994.

A detailed description of the adaptations to TOMS for Meteor-3 is provided by Herman *et al.* (1996) and pre-launch and post-launch calibrations are described by Jaross *et al.* (1995). As a result of post-launch calibration it was found that there was severe degradation of an aluminum diffuser plate deployed to reflect sunlight into the instrument. On board Nimbus-7 severe degradation of the diffuser plate was also observed as time passed (Wellemeyer *et al.*, 1996). The three-diffuser system aboard Meteor-3 reduced the exposure and degradation of the diffuser and allowed calibration by comparing signals reflected by diffusers with different rates of exposure. As mentioned above, diffusers were arranged along the sides of an equilateral triangle

and mounted on a carousel, so that a given diffuser could be placed into view on demand. For Meteor-3 TOMS TOC the absolute error is  $\pm 3\%$  and the drift for 40 months is less than  $\pm 1\%$ . Meteor-3 TOMS agrees with both Nimbus-7 TOMS and ground-based measurements to better than 1% (McPeters *et al.*, 1996).

Of the five TOMS instruments that were built, four entered successful orbit. Nimbus-7 and Meteor-3 provided global measurements of total column ozone on a daily basis and together provided a complete dataset of daily ozone from November 1978–December 1994. After an 18-month period when the program had no on-orbit capability, ADEOS TOMS (see Section 2.3.3) was launched on August 17, 1996 and provided data until the satellite which housed it lost power on June 29, 1997. Earth Probe TOMS was launched on July 2, 1996 to provide supplemental measurements, but was boosted to a higher orbit to replace the failed ADEOS. The transmitter for the Earth Probe TOMS failed on December 2, 2006. Since January 1, 2006 data from the Ozone Monitoring Instrument (OMI, see Section 2.3.2) has replaced Earth Probe TOMS.

Their historical and current daily and monthly data are widely available at the NASA website <http://toms.gsfc.nasa.gov> Spatially, a good global coverage in TOMS (OMI) data is combined with a high resolution of  $1^\circ$  by latitude and  $1.25^\circ$  by longitude (McPeters *et al.*, 1998).

In addition to ozone, the TOMS instrument measures sulfur dioxide released in volcanic eruptions. These observations are of great importance in the detection of volcanic ash clouds that are hazardous to commercial aviation.

### 2.3.2 Ozone Monitoring Instrument (OMI)

The OMI instrument mentioned above is a nadir-viewing near-UV/visible CCD spectrometer aboard NASA's Earth Observing System's (EOS) Aura satellite. Aura flies in formation about 15 minutes behind Aqua, both of which orbit the Earth in a polar Sun-synchronous pattern. Aura was launched on July 15, 2004 and the OMI has collected data since August 9, 2004. The other instruments flown on Aura include HIRDLS (see Section 2.5.3.8), MLS (see Section 2.5.3.4), and TES (see Section 2.5.3.5).

OMI measurements cover a spectral region of 264–504 nm with a spectral resolution between 0.42 nm and 0.63 nm and a nominal ground footprint of  $13 \text{ km} \times 24 \text{ km}$  at nadir (see Table 2.3). Essentially complete global coverage is achieved in one day. The significantly improved spatial resolution of OMI measurements as well as the vastly increased number of wavelengths observed—as compared to TOMS, GOME (Global Ozone Monitoring Experiment), and SCIAMACHY (SCanning Imaging Absorption Spectrometer for Atmospheric Chartography)—sets a new standard for trace gas and air quality monitoring from space. OMI observations provide the following capabilities and features:

- mapping of ozone columns at  $13 \text{ km} \times 24 \text{ km}$  and profiles at  $13 \text{ km} \times 48 \text{ km}$  (a continuation of TOMS and GOME ozone column data records and the ozone profile records of SBUV and GOME);

**Table 2.3.** General description of OMI (OMI, 2009).

<i>Parameter</i>	<i>Value</i>
Wavelength range:	UV-1: 264–311 nm UV-2: 307–383 nm VIS: 349–504 nm
Spectral resolution (FWHM)	UV-1: 0.63 nm UV-2: 0.42 nm VIS: 0.63 nm
Spectral sampling (FWHM)	UV-1: 1.9 px UV-2: 3.0 px VIS: 3.0 px
Telescope FOV	115° (2,600 km on ground)
IFOV	12 km × 6 km (flight direction × cross-flight direction)
Detector	CCD: 780 × 576 (spectral × spatial) pixels
Mass	65 kg
Duty cycle	60 minutes on daylight side 10–30 minutes on eclipse side (calibration)
Power	66 W
Data rate	0.8 Mbps (average)

- measurement of key air quality components: NO<sub>2</sub>, SO<sub>2</sub>, BrO, HCHO, and aerosol (a continuation of GOME measurements);
- ability to distinguish between aerosol types, such as smoke, dust, and sulfates;
- the ability to measure aerosol absorption capacity in terms of aerosol absorption optical depth or single-scattering albedo;
- measurement of cloud pressure and coverage;
- mapping of the global distribution and trends in UV-B radiation;
- combining processing algorithms including TOMS Version 8, DOAS (Differential Optical Absorption Spectroscopy, see Section 1.5), hyperspectral BUV retrievals, and forward modeling to extract the various OMI data products;
- near real-time measurements of ozone and other trace gases.

OMI's scientific mission objectives (discussed in detail by Levelt *et al.*, 2006) were directly related to the Aura mission objectives. The OMI mission seeks answers to the following questions:

- Is the ozone layer recovering as expected?
- What are the sources of aerosols and trace gases that affect global air quality and how are they transported?
- What are the roles of tropospheric ozone and aerosols in climate change?
- What are the causes of surface UV-B change?

The OMI employs hyperspectral imaging to observe solar backscatter radiation in the visible and ultraviolet improving the accuracy and precision of the TOC amounts and also allow for accurate radiometric and wavelength self-calibration over the long term. The instrument observes Earth's backscattered radiation with a wide-field telescope feeding two imaging grating spectrometers. It is a contribution of the NIVR (Netherlands Institute for Air and Space Development) of Delft, in collaboration with the Finnish Meteorological Institute (FMI), to NASA's Aura mission. The Dutch industrial efforts focused on the optical bench design and assembly, thermal design, and project management. The detector modules and the readout and control electronics were provided by Finnish industrial partners. An extensive discussion of the OMI can be found in the *OMI User's Guide* (OMI, 2009). It can distinguish between aerosol types, such as smoke, dust, and sulfates, and measures cloud pressure and coverage, which provide the data necessary to derive tropospheric ozone. OMI continues the TOMS record for total ozone and other atmospheric parameters related to ozone chemistry and climate (<http://www.itc.nl/research/products/sensordb/AllSensors.aspx>).

Ozone profiles have been derived from the BUV/SBUV series of instruments since the 1970s. However, vertical ozone information is limited to above about 25 km because of the selection of the 12 wavelengths used by these instruments. Using hyperspectral OMI measurements (270–330 nm), ozone vertical profiles from the surface to about 60 km are derived at high spatial resolution (13 km × 48 km at nadir) and with daily global coverage. The retrieved ozone profiles agree very well with Microwave Limb Sounder (MLS) (see Section 2.5.3.4) measurements; the global mean biases are within 2.5% above 100 hPa and 5–10% below 100 hPa (for further details see Liu *et al.*, 2010).

Veefkind *et al.* (2006) described an algorithm for deriving total column ozone from spectral radiances and irradiances measured by the Aura OMI; this algorithm is based on the differential optical absorption spectroscopy (DOAS, see Section 1.5) technique. The main characteristics of the algorithm and an error analysis are described. The algorithm was successfully applied to the first available OMI data and comparisons with data from ground-based instruments were very encouraging and clearly showed the potential of the method.

The Aura satellite that carries the OMI has the capability to directly broadcast measurements to ground stations at the same time as measurements are being stored in the spacecraft's memory for later transmission to Earth. The Finnish Meteorological Institute's very fast delivery (VFD) processing system utilizes this direct broadcast to produce maps of total ozone and ultraviolet radiation over Europe within 15 minutes of the satellite overpass of the Sodankylä ground station in northern Finland. VFD products include maps of total ozone, ultraviolet index, and

ultraviolet daily dose. The aim of this service is to provide up-to-date information on the ozone and ultraviolet situation for the general public and snapshots of the current situation for scientists. The accuracy of VFD products compares well with standard off-line OMI ozone products and ground-based Brewer measurements (Hassinen *et al.*, 2008; Ialongo *et al.*, 2008).

### 2.3.3 Advanced Earth Observing Satellite (ADEOS I, II)

The Japanese ADEOS carried the fourth TOMS into orbit on August 17, 1996. It remained in range between 10:45 AM to 11:45 AM throughout the ozone data record from September 11, 1996 to June 29, 1997. Its orbital inclination was  $98.6^\circ$  and the nominal orbit altitude was 800 km with a period of 100.9 min.

The approach taken to calibrate the three diffuser plates (by examining the differences in degradation of diffuser reflectivity resulting from the different rates of exposure) was first used with Meteor-3 TOMS and proved to be successful. In addition the Japanese ADEOS/TOMS is equipped with UV lamps for monitoring the reflectivity of the solar diffusers.

For ADEOS/TOMS TOC, the absolute error was  $\pm 3\%$ , the random error is  $\pm 2\%$ , and the drift over the 9-month data record was less than  $\pm 0.5\%$ .

The ADEOS/TOMS observations of TOC are approximately 1.5% higher than a 45-station network of ground-based measurements (Herman *et al.*, 1997; Krotkov *et al.*, 1998; McPeters and Labow, 1996; Seftor *et al.*, 1997; Torres and Bhartia, 1999; Torres *et al.*, 1995).

The complementary instrumentation of ADEOS includes the Improved Limb Atmospheric Spectrometer (ILAS), the Interferometric Monitor for Greenhouse Gases (IMG), and the Retro-reflector In Space (RIS) instrument. ILAS is described in Section 2.5.3.10. IMG is a nadir-observing Michelson-type FTS (see Sections 1.5.4 and 2.3.10) designed to measure the density profiles of  $\text{CO}_2$  and  $\text{H}_2\text{O}$ , total ozone column, and mixing ratios of  $\text{CH}_4$ ,  $\text{N}_2\text{O}$ , and CO in the troposphere. The RIS, which is used together with laser ground stations, supports vertical profile and/or column measurements of a small number of gases.

ADEOS-II (a Sun-synchronous orbit satellite) launched by NASDA, NASA, and CNES in December 2002 was developed to include sensors like the Advanced Microwave Scanning Radiometer (AMSR), an advanced microwave radiometer developed by the National Space Development Agency of Japan (NASDA). It was equipped with the Improved Limb Atmospheric Spectrometer-II (ILAS-II), an improved spectrometer for measuring infrared radiation at the edge of the atmosphere, which was developed by the Environmental Agency of Japan (Kondratyev *et al.*, 1998). The mission ended in October 2003 after the satellite's solar panels failed ([http://www.jaxa.jp/projects/sat/adeos2/index\\_e.html](http://www.jaxa.jp/projects/sat/adeos2/index_e.html)).

### 2.3.4 Solar Backscattered Ultraviolet Radiometer (SBUV)

We now move on to consideration of the SBUV instruments. The SBUV instruments are nadir-viewing instruments that determine total column ozone and the ozone



vertical profile by measuring sunlight scattered from the atmosphere in the ultra-violet spectrum. As we did much earlier on in the case of temperature sounding, we assume that the atmosphere is infinitely deep so that the ground can be neglected.

The Nimbus series of satellites, starting with Nimbus-4 in 1970, was used to measure global distributions of ozone for seven years, using the backscattered ultra-violet (BUV) technique, which is briefly described here. Incident solar radiation at 317.5 and 360 nm passes through the ozone within the upper atmosphere and is backscattered largely within the troposphere at altitudes below the peak in ozone concentration. This backscattered radiation passes once again through the ozone to the satellite. The radiation at 317.5 nm is attenuated by ozone during both passages through the atmosphere. However, measurements at the 317.5 nm BUV alone cannot be used to determine TOC without knowledge of the varying reflectivity of the backscattering region. In order to determine this reflectivity, the 360 nm BUV (which is not attenuated by ozone), is measured with the BUV technique. The first synoptic global images of TOC were obtained in the sunlit hemisphere, using the imaging instrumentation on board the *Dynamics Explorer-1* (DE-1) spacecraft. The first instrument in this series was the Backscatter Ultraviolet (BUV) instrument which was flown on NASA's Nimbus-4 satellite, which was launched in 1970. It was in operation until 1977, but not continuously due to spacecraft power problems. An improved version, the Solar Backscatter Ultraviolet radiometer (SBUV) was flown on Nimbus-7 which was launched in 1978. This was followed by the SBUV/2 on the NOAA-9, -11, -14, -16, and -17 satellites (see [Table 2.4](#)).

The BUV instrument is a downward-viewing double monochromator with a 1 nm bandpass, which is stepped through 12 wavelength increments every 32 s through the 255–340 nm spectral region. In addition, there is a separate filter photometer with a 5 nm bandpass centered at 380 nm, which is used to measure backscattered radiance. This instrument was designed to determine the vertical ozone profile, while measuring backscattered solar UV radiation directed vertically upwards from the ground. Two wavelength pairs are used for measuring total ozone, and eight short wavelengths are used to profile the ozone. The precision of this instrument is better than 2% for zenith angles less than about 60° and clear conditions. The accuracy is limited to approximately 6%.

The SBUV instruments—starting with the SBUV on Nimbus-7—are all of similar design: nadir-viewing double-grating monochromators of the Ebert–Fastie type. The instruments use 12 narrow bands in the wavelength range 0.25–0.34  $\mu\text{m}$ , using sunlight or moonlight, while viewing the Earth in the fixed nadir direction with an instantaneous field of view (IFOV) on the ground of approximately 180 km  $\times$  180 km. The spectral resolutions for the SBUV(/2) monochromators are all approximately 1.1 nm. The wavelength channels used for Nimbus-7 SBUV were very similar to those of the SBUV/2 (see [Table 2.5](#)), except that on Nimbus-7 channel 1 had been at 256 nm. This was moved to 252.0 nm on the SBUV/2 in order to avoid emission in the nitric oxide gamma band that contaminated the SBUV channel 1 measurement.

The total ozone algorithm uses the four longest wavelength bands (312.57, 317.56, 331.26, and 339.89 nm), whereas the profiling algorithm uses the shorter

**Table 2.4.** Satellite instrumentation for BUUV ozone observations (Hilsenrath *et al.*, 1997).

<i>Instrumentation</i>	<i>Satellite</i>	<i>Observation period</i>
BUV	Nimbus-4	1970–1975
SBUV	Nimbus-7	1979–1990
SBUV/2	NOAA-9	1985–1998
SBUV/2	NOAA-11	1989–2003
SBUV/2	NOAA-14	1995–present
SBUV/2	NOAA-16	2000–present
SBUV/2	NOAA-17	2002–present
SSBUV	Shuttle	8 flights, 1989–1996
TOMS	Nimbus-7	1978–1993
TOMS	Meteor-3M	1991–1994
TOMS	Earth Probe	1996–2005
TOMS	ADEOS	1996–1997
GOME	ERS-2	1995–present
Aura	OMI TO3	2004–present
IASI	MetOp	2006–present
GOME 2	MetOp	2006–present

wavelengths. Ozone profiles and total column amounts are derived from the ratio of observed backscattered spectral radiance to incoming solar spectral irradiance. This ratio is referred to as the “backscattered albedo”. The only difference in the optical components between radiance and irradiance observations is the instrument diffuser used to make the solar irradiance measurement; the remaining optical components are identical. Therefore, a change in diffuser reflectivity will result in an apparent trend in ozone.

The Shuttle Solar Backscatter Ultraviolet Spectral Radiometer (SSBUV) was designed and developed at Goddard Space Flight Center to calibrate the Nimbus and NOAA instruments. It carries out measurements of ozone concentrations by comparing solar ultraviolet radiation with that scattered back from the atmosphere. In late 1989, the Space Shuttle *Atlantis* carried the instrument for the first time, in an appropriate orbital flightpath to assess performance by directly comparing data from

identical instruments (SBUV) on board the NOAA spacecraft and the Nimbus-7. The Shuttle SBUV (SSBUV) was flown on eight missions between October 1989 and January 1996 and provided regular checks on individual satellite instrument calibrations. Multiple intercomparisons with ground-based instruments have improved data retrieval algorithms and, therefore, satellite ozone measurements have become compatible with those of the network of ground-based measurements. The principal purpose was to compare observations from several ozone-measuring instruments on board NOAA-9, NOAA-11, Nimbus-7, and UARS; this was because of the degradation of SBUV and SBUV/2 instruments in space. The quality of in-orbit calibration depends on the flight-to-flight calibration repeatability in SSBUV. Given accurate measurements of backscattered radiance, it is necessary to account for differences in solar zenith angle and effective surface reflectivity (Heath *et al.*, 1993) (see Section 3.2 for a further discussion of the intercomparison of different instruments).

A UV spectrometer was also flown aboard the EXOS-C/Ohzora satellite (launched in February 1984) to measure backscattered UV in the wavelength region 250–320 nm with a spectral resolution of 1 nm for the period March 1984–September 1987 (Ogawa *et al.*, 1989). Complete global coverage of total ozone was obtained. However, an anomaly in the Earth's magnetic field in the South Atlantic affects the distribution of Van Allen radiation belts and, therefore, these radiation levels send too much noise to the detectors. This was overcome in the Solar Backscattered UV instrument (SBUV) by adding a 50 Hz optical chopper.

**Table 2.5.** SBUV/2 wavelengths (NOAA, 2009).

<i>Channel</i>	<i>Wavelength (nm)</i>
1	252.00
2	273.61
3	283.10
4	287.70
5	292.29
6	297.59
7	301.97
8	305.87
9	312.57
10	317.56
11	331.26
12	339.89

### 2.3.5 Global Ozone Monitoring Experiment (GOME)

GOME was launched in 1995 aboard the ESA's Earth Resources Satellite (ERS-2) in a polar Sun-synchronous orbit. It is a nadir-viewing multichannel spectrometer measuring solar irradiance and upwelling radiance (backscattered from the atmosphere and earthshine radiance) in the wavelength range 240–790 nm at moderate spectral resolution (0.2–0.4 nm). The four main channels provide continuous spectral coverage of the wavelengths between 240 and 790 nm (channel 1: 237–314 nm,

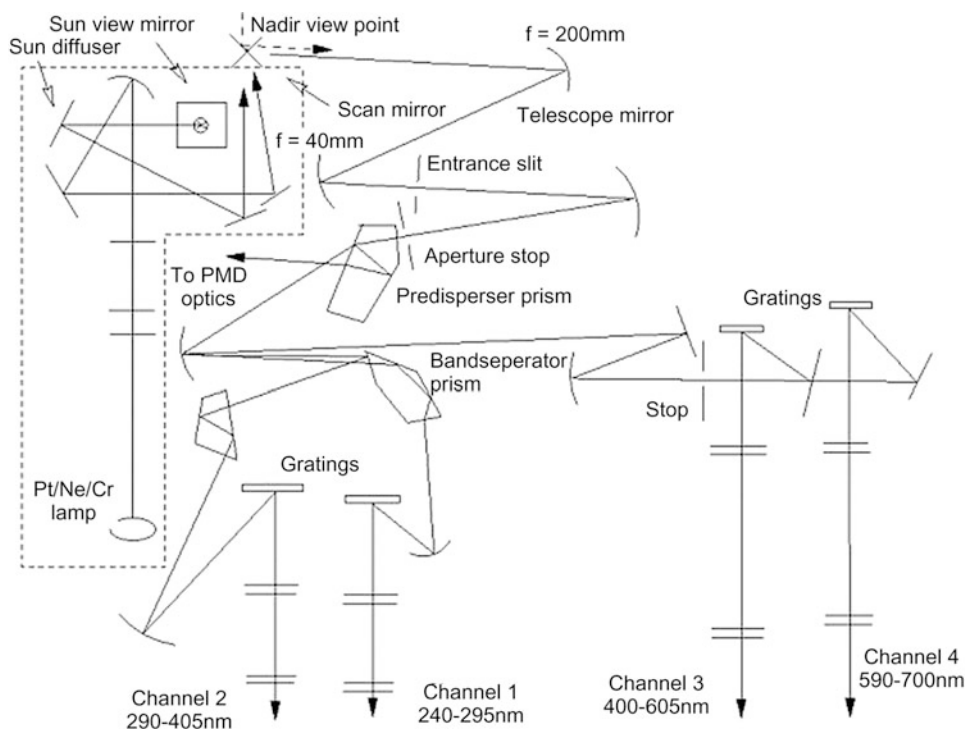


**Figure 2.3.** Schematics of GOME Optics. The GOME instrument is a four-channel spectrometer. Adjacent to the spectrometer is a calibration unit housing a Pt/Cr/Ne hollow cathode discharge lamp and the fore optics for solar viewing (Weber *et al.*, 1998).

channel 2: 311–405 nm, channel 3: 410–600 nm, channel 4: 610–790 nm) (see Figure 2.3). The instrument exploits the fact that near 260 nm the penetration depth of solar radiation into the atmosphere strongly increases with increasing wavelength, because at this specific wavelength the ozone absorption cross-sections have their maximum. When radiation has a wavelength greater than about 310 nm, it penetrates the tropopause reaching the surface. Therefore, the measurement of backscattered radiation in the UV–visible region provides information about the vertical ozone concentration profile. In general, GOME measures the TOC, ozone vertical profile, and total column of several trace constituents, including BrO, NO<sub>2</sub>, and ClO<sub>2</sub> and also obtains information on clouds, aerosols, and surface spectral reflectance. It can measure TOC at a higher horizontal resolution than TOMS and, thus, complements TOMS observations. Retrieval of OVP from backscattered UV–visible spectra is based on the “eigenvector method”, which uses *a priori* information (climatological mean profile with the corresponding covariance matrix) as the original optimal estimation approach.

Alternatively, the Full Retrieval Method (FURM), which was developed at the Institute of Remote Sensing of the University of Bremen, can be used. This is mainly

based on the optimal estimation approach and contains the radiative transfer code GOMETRAN as an essential tool (Rozanov *et al.*, 1997, 1998). An explicit treatment of clouds in the retrieval algorithm based on a new GOMETRAN cloud parameterization has been developed by Kurosu *et al.* (1997). An advanced radiative transfer model, SCIATRAN, has been developed by Rozanov *et al.* (2002) mainly for the retrieval of atmospheric constituents from global nadir radiance measurements of the SCIAMACHY satellite spectrometer. This is a further development of the successful GOMETRAN. SCIATRAN solves the radiative transfer equation using the Finite Difference Method for a plane-parallel vertically inhomogeneous atmosphere taking into account multiple scattering.

A second GOME-2 instrument was flown on MetOp-1, ESA's first polar-orbiting meteorological satellite which was launched on October 16, 2006. GOME-2 on the satellites ERS-2 and MetOp 1 operates in four bands—band 1: 240 to 295 nm, band 2: 290 to 405 nm, band 3: 400 to 605 nm, band 4: 590 to 790 nm; these are slightly different from the bands on GOME-1 (launched on April 20, 1995) (<http://rammb.cira.colostate.edu/dev/hillger/ozone-monitoring.htm>). Some early work on comparison of its TOC data with reliable ground-based measurements recorded by five Brewer spectroradiometers in the Iberian Peninsula was described by Antón *et al.* (2009). A similar comparison for the predecessor instrument GOME/ERS-2 is also described. The period of study was a whole year from May 2007 to April 2008. The results show that GOME-2/MetOp ozone data are already of very good quality. TOC values were found to be on average 3.05% lower than Brewer measurements. This underestimation is higher than that obtained for GOME/ERS-2 (1.46%). However, the relative differences between GOME-2/MetOp and Brewer measurements show significantly lower variability than the differences between GOME/ERS-2 and Brewer data. The dependences of these relative differences on satellite solar zenith angle (SZA), satellite scan angle, satellite cloud cover fraction (CF), and ground-based total ozone measurements were analyzed. For both GOME instruments, the differences show no significant dependence on solar zenith angle. However, GOME-2/MetOp data show a significant dependence on satellite scan angle (+1.5%). In addition, GOME/ERS-2 differences present a clear dependence on CF and ground-based total ozone; such differences are minimized for GOME-2/MetOp. The comparison between the daily total ozone values provided by both GOME instruments shows that GOME-2/MetOp ozone data are on average 1.46% lower than GOME/ERS-2 data without any seasonal dependence. Finally, deviations of the *a priori* climatological ozone profile used by the satellite retrieval algorithm from the true ozone profile are analyzed. Although excellent agreement between *a priori* climatological and measured partial ozone values is found for the middle and high stratosphere, relative differences greater than 15% are common for the troposphere and lower stratosphere.

### 2.3.6 ESA ENVISAT, GOMOS

Among the many instruments on ENVISAT launched by the European Space Agency (ESA) the Global Ozone Monitoring by Occultation of Stars (GOMOS)

instrument is relevant to stratospheric ozone measurements (Megie *et al.*, 1989). It is a stellar occultation instrument onboard the ENVISAT satellite (see Bertaux *et al.*, 1991, 2000a, b, 2004, 2010; ESA, 2003, <http://envisat.esa.int/handbooks/gomos/>; Kyrölä *et al.*, 2004) (see Section 1.7.4.1). GOMOS measurements start at an altitude of 130 km and the first few measurements are used to determine a star's undisturbed spectrum (the reference spectrum). Horizontal transmission spectra are calculated from the star spectra measured through the atmosphere and the reference spectrum. The integration time is 0.5 s, which gives an altitude-sampling resolution of 0.5–1.6 km depending on the tangent altitude and the azimuth angle of the measurement. GOMOS measures both during the day and night (Kyrölä *et al.* 2006).

The spectral ranges of GOMOS detectors are 248–690 nm, 755–774 nm, and 926–954 nm, which make it possible to retrieve the vertical profiles of O<sub>3</sub>, NO<sub>2</sub>, NO<sub>3</sub>, H<sub>2</sub>O, O<sub>2</sub>, and aerosols. For O<sub>3</sub> they are retrieved from the UV–visible spectral range 248–690 nm. Retrieved ozone profiles have 2 km vertical resolution below 30 km and 3 km above 40 km. Retrieval algorithm details and data quality are discussed by Kyrölä *et al.* (2010b) and Tamminen *et al.* (2010), <http://envisat.esa.int/dataproducts/gomos>. Retrieved ozone distributions for 2002–2008 are described by Kyrölä *et al.* (2006, 2010a).

### 2.3.7 The Ozone Mapping and Profiler Suite (OMPS) and the NPOESS

The Ozone Mapping and Profiler Suite (OMPS) is one of the five instruments to be included in the U.S. National Polar-orbiting Operational Environmental Satellite System (NPOESS). For many years two parallel and rather similar, but not identical, polar-orbiting meteorological satellite programs were run by the National Oceanic and Atmospheric Administration (NOAA) and the DoD (Department of Defense). NASA had also been involved, in various ways, in a variety of polar-orbiting environmental remote-sensing programs.

NPOESS was planned as a tri-agency program with the Department of Commerce (specifically NOAA), the Department of Defense (DoD, specifically the Air Force), and NASA. It was designed to merge the civil and defense weather satellite programs of the NOAA Polar Operational Environmental Satellites (POES) series and the U.S. Department of Defense's Defense Meteorological Satellite Program (DMSP), respectively, in order to reduce costs and to provide global weather and climate coverage with improved capabilities over the earlier systems. NPOESS was to be the United States' next-generation satellite system that would monitor the Earth's weather, atmosphere, oceans, land, and near-space environment. NPOESS satellites were to host proven technologies and operational versions of sensors that were under operational prototyping by NASA.

The NPOESS Preparatory Project (NPP) program aimed to bridge the gap between the old and the new systems by flying new instruments on a satellite originally to be launched in 2005. However, the program encountered technical, financial, and political problems leading to a delay of the launch of NPP until 2011 (NPP was successfully launched on October 28, 2011) and of the launch of the first NPOESS platform (C-1) until late 2014. These would each constitute delays of about five years



from the original plan. This led to a review of the NPOESS, and as a result of this review the White House announced on February 1, 2010 that the NPOESS satellite partnership was to be dissolved. Two separate lines of polar-orbiting satellites to serve military and civilian users would be pursued instead:

- The NOAA/NASA portion is called the “Joint Polar Satellite System” (JPSS). The JPSS-1 spacecraft will be constructed by Ball Aerospace & Technologies Corp. under a fixed price contract of \$248 million with a performance period to February 1, 2015.
- The Defense Department’s portion is called the “Defense Weather Satellite System” (DWSS).

The existing partnership with Europe through the European Organization for the Exploitation of Meteorological Satellites (EUMETSAT), which operates the MetOp polar-orbiting weather satellite program, would continue.

The five-instrument suite for NPOESS includes the Visible/Infrared Imager Radiometer Suite (VIIRS), the Cross-track Infrared Sounder (CrIS), the Clouds and the Earth Radiant Energy System (CERES), the Advanced Technology Microwave Sounder (ATMS), and the Ozone Mapping and Profiler Suite (OMPS). OMPS was designed to monitor ozone from space. It is comprised of two sensors, a nadir sensor and a limb sensor. Measurements from the nadir sensor are used to generate total column ozone measurements, while measurements from the limb sensor generate the ozone profiles of along-track limb-scattered solar radiance. OMPS will make measurements used to generate estimates of total column and vertical profile ozone data. These will continue the daily global data produced by the current ozone-monitoring systems, the Solar Backscatter Ultraviolet radiometer (SBUV)/2, and the Total Ozone Mapping Spectrometer (TOMS), but with higher fidelity. Collection of these data contributes to fulfilling the U.S. treaty obligation to monitor ozone depletion for the Montreal Protocol to ensure there are no gaps in ozone coverage.

OMPS consists of two telescopes, a nadir one and a limb one, feeding three detectors. The instruments use a configuration of working and reference solar diffusers to maintain calibration. The nadir sensor uses a wide-field-of-view push-broom telescope to feed two separate spectrometers. The nadir total column spectrometer measures scene radiance from 300 to 380 nm with a resolution of 1 nm sampled at 0.42 nm. Measurements from this spectrometer will be used to generate TOC with daily coverage of the sunlit Earth to continue heritage records from the Total Ozone Mapping Spectrometer (TOMS). The performance specifications for total column ozone Environmental Data Records (EDRs) from OMPS Nadir Mapper measurements are identified in table 2 of Flynn *et al.* (2009). The NPOESS algorithm is an extension of the TOMS Version 7 total ozone algorithm (McPeters and Labow, 1996). It uses multiple triplets of measurements: one chosen for ozone sensitivity, a second chosen to give an estimate of cloud and surface reflectivity, and a third to estimate the variation of reflectivity with wavelength. The triplets used in the final ozone estimates are selected so that the ozone-sensitive



channels maintain sensitivity to the column as the solar zenith angle and column amount vary.

The OMPS nadir telescope also feeds a nadir profile grating spectrometer. It will measure from 250 to 310 nm with a 1.1 nm FWHM bandpass and 0.4 nm sampling and a 250 by 250 km<sup>2</sup> nadir-only FOV. These measurements will be used to continue the SBUV/2 ozone profile record. Ozone profile estimates will be obtained from the Version 8 SBUV/2 ozone profile retrieval algorithm with adaptations to use the increased number of wavelengths present in OMPS Nadir Profiler measurements. The OMPS limb sensor measures along-track limb-scattered solar radiance with 1 km vertical sampling in the spectral range from 290 to 1,000 nm. Three vertical slits sample the limb spaced at 250 km cross-track intervals to provide for weekly global coverage. The limb instrument will be flown as an experimental component on the NPP mission but is not currently manifested for future NPOESS satellites. The capabilities and complexities of retrieving ozone profiles from limb measurements are analyzed by Loughman *et al.* (2005).

### 2.3.8 Ozone Dynamics Ultraviolet Spectrometer (ODUS)

This is a Japanese ultraviolet instrument measuring ozone and several other species (e.g., O<sub>3</sub>, SO<sub>2</sub>, and NO<sub>2</sub> in urban polluted air, BrO, and OClO, aerosols) in the troposphere and stratosphere. ODUS uses techniques similar to those used by TOMS and GOME (see Sections 2.3.1 and 2.3.5) launched on the GCOM-A1 platform (2007–2012).

### 2.3.9 Ozone Layer Monitoring Experiment (OLME)

This instrument consists of UV cameras using both charge-coupled devices and UV photodiode detectors. It was flown aboard Chile's FaSAT Bravo satellite in 1997 and measured ozone in the Antarctic and sub-Antarctic regions of Chile. Another instrument, the OM-2 (developed in Israel), uses filters for the measurement of total ozone and the ozone vertical profile aboard the Israeli Techsat-1 satellite (Parnes, 1992).

### 2.3.10 Interferometric Monitor for Greenhouse Gases (IMG)

This is a Michelson-type interferometer which was launched on August 17, 1996 on the Japanese ADEOS platform. This instrument monitors IR spectra (3.3–14 μm) from the Earth's surface and the atmosphere, observing with a nadir view. For data inversion the atmospheric temperature profile is needed in order to retrieve the total amounts of O<sub>3</sub>, CO, and CH<sub>4</sub>, and a few points of the vertical profile. For these data an inversion algorithm based on neural network techniques is currently used (Hadji-Lazaro *et al.*, 1998).

### 2.3.11 Infrared Atmospheric Sounding Interferometer

This instrument is a Michelson-type interferometer providing spectra between 3.4 and 15.5  $\mu\text{m}$ , with an apodized resolution of  $0.5\text{ cm}^{-1}$  (Hadj-Lazaro *et al.*, 1998). The total amount of ozone under cloud-free conditions is measured with a horizontal resolution of 25 km and an accuracy of 5%. It was launched on October 19, 2006 on the satellite MetOp-1.

Let us briefly discuss some results illustrating TOC observations (some more results will be considered in Chapter 3).

## 2.4 OBSERVED VARIABILITY IN TOTAL OZONE COLUMN

The TOC is characterized by significant spatiotemporal variability. As far as temporal variability is concerned, it consists of large periodic and aperiodic components. Periodic variations have timescales ranging from day-to-day changes, through seasonal and annual variations, to an 11-year solar cycle. Aperiodic variations include the irregular Quasi-Biennial Oscillation (QBO) with a period of roughly 26–30 months, the irregular El Niño Southern Oscillation (ENSO) with a period of 4–7 years, and other interannual signals. Ozone trends are important phenomena that will be considered in Chapters 4 and 6.

As far as spatial variability is concerned, it is characterized by latitudinal and longitudinal dependence. Satellite systems for studying atmospheric ozone have the advantage that they provide frequent (near) global coverage, whereas traditional ground-based and ozonesonde measurements only provide data at a small number of locations. As we shall see in Chapter 3, the algorithms that are used in processing satellite data need to be validated and refined by comparison with the results of more conventional measurements. In the meantime we discuss the spatial variations in TOC that are revealed by satellite data.

### 2.4.1 Latitudinal variation of TOC

A very important feature of global TOC distribution is the strong latitudinal gradient with lower values over the equator and tropics and higher values over mid and high latitudes. This gradient is characterized by a well-pronounced annual cycle, reaching a maximum in spring and a minimum in autumn. The amplitude of this annual cycle is a function of latitude, with a maximum at about  $60^\circ$  north and south latitude (Varotsos *et al.*, 2000). In the tropics seasonal variations are small, with ozone maxima in summer. Such a latitudinal distribution results from the relatively long lifetime (months to years) of ozone in the lower stratosphere and the Brewer–Dobson circulation that transports stratospheric ozone from the tropics toward the poles and downwards at high latitudes.

Bojkov and Fioletov (1995), based on re-evaluated TOC observations from over 100 Dobson and filter radiometer stations from pole to pole, presented the following TOC trend results:

- Up to 1995 TOC continued its decline (which started in the 1970s), with statistically significant year-round and seasonal trends except over the equatorial belt.
- The cumulative year-round TOC reduction over the 35°–60° belts of both hemispheres since the early 1970s is close to 8%. In the southern mid-latitudes, it is difficult to distinguish the seasonal dependence of TOC trends, while the cumulative decline in the northern mid-latitudes in winter and spring is about 9% and 4–6% for summer and autumn.
- Observations from 12 Dobson polar stations have demonstrated that the northern polar region shows the same ozone decline as northern mid-latitudes or even a slightly stronger one (the cumulative decline is about 7% year-round and 9% for winter and spring). In the southern polar region the December–March trend is also nearly the same as the mid-latitude trend reaching about 10%, while during September–November the decline reaches 40%.
- The eruption of Mount Pinatubo in 1991 did not significantly influence overall declining TOC trends.
- TOC trends are likely to continue until the peak levels of chlorine are reached in the stratosphere.

It appears that more recent volcanic eruptions than Mount Pinatubo have no long-term effects on TOC (Clarisse *et al.*, 2008; Flentje *et al.*, 2010).

The TOC trends for various geographic regions for January 1979 to March 1995 are shown in Table 2.6 (Bojkov and Fioletov, 1998).

The afore-mentioned results provide the observed TOC variability which marked the beginning of the TOC depletion phenomenon. Nowadays, according

**Table 2.6.** TOC trends for January 1979 to March 1995 for five regions of northern mid-latitudes, the Arctic, and Antarctica (Bojkov and Fioletov, 1998).

	<i>Trend</i> (%/decade)			
	<i>Year</i>	<i>Dec.–Mar.</i>	<i>May–Aug.</i>	<i>Sep.–Nov.</i>
North America (36°–60°N)	$-4.2 \pm 1.4$	$-4.5 \pm 2.2$	$-4.5 \pm 1.9$	$-2.6 \pm 1.4$
Europe (40°–60°N)	$-4.8 \pm 1.6$	$-7 \pm 3.2$	$-4.3 \pm 1.9$	$-1.7 \pm 2.0$
European Russia (45°–60°N)	$-4.4 \pm 1.6$	$-6.3 \pm 3.0$	$-2.8 \pm 1.9$	$-2.1 \pm 1.8$
Western Siberia (50°–60°N)	$-5.8 \pm 1.7$	$-8.2 \pm 3.1$	$-3.6 \pm 1.9$	$-3.6 \pm 2.1$
Eastern Siberia and Far East (43°–62°N)	$-6.4 \pm 1.7$	$-7.8 \pm 2.3$	$-5.2 \pm 2.4$	$-5.7 \pm 2.2$
Arctic (60°–80°N)	$-5.3 \pm 1.7$	$-7.7 \pm 3.2$	$-3.8 \pm 1.9$	$-2.5 \pm 2.2$
Antarctica (65°–90°S)		$-5.4 \pm 3.0$		$-22 \pm 8$

to the recent scientific ozone assessment (WMO, 2010a), the average total ozone values in 2006–2009 remain at roughly 3.5% and 2.5% below the 1964–1980 averages, respectively, for 90°S–90°N and 60°S–60°N. Mid-latitude (35°–60°) annual mean TOC amounts in the Southern Hemisphere (Northern Hemisphere) over the period 2006–2009 have remained at the same level as observed during 1996–2005: at ~6% (~3.5%) below the 1964–1980 average. The TOC decline in Arctic winter and spring between 2007 and 2010 has been variable, but has remained in a range comparable to the values prevailing since the early 1990s. In addition, springtime Antarctic TOC losses continue to occur every year. Although ozone losses exhibit year-to-year variations that are primarily driven by year-to-year changes in meteorology, the October mean TOC within the vortex has been about 40% below 1980 values for the past 15 years. In other words, the springtime Antarctic TOC does not yet show a statistically significant increasing trend.

As far as the future projection is concerned, the global annually averaged TOC is expected to return to 1980 levels before the middle of the century and before stratospheric halogen loading returns to 1980 levels. Global (90°S–90°N) annually averaged TOC will likely return to 1980 levels between 2025 and 2040, well before the return of stratospheric halogens to 1980 levels between 2045 and 2060. Simulated changes in tropical TOC from 1960 to 2100 are generally small.

Chandra *et al.* (1996) and Varotsos *et al.* (1997a, b), using measurements of TOC by Nimbus-7 TOMS version 7, suggested that trends over the latitudes centered at 40°N in the Northern Hemisphere vary from –3 to –9% per decade during winter and within –2 to –3% per decade during summer.

To account for the effects of dynamical perturbations on TOC Chandra *et al.* (1996) used tropospheric or stratospheric temperature as an index of dynamical variability. Figure 2.4 depicts the relative changes in regional and local trends, with respect to zonal mean trends. The regional and zonal trends chosen correspond to the Mediterranean region (35–45°N, 0–30°E) and Athens, Greece (38°N, 24°E). This figure also shows the ranges (shaded area) in seasonal trends over the longitude circle at 40°N derived from TOMS data. Figure 2.4a is based on the linear regression model which includes the QBO signal (based on the 30 hPa Singapore zonal wind) and the solar cycle signal (based on F10.7 radio emission flux at the wavelength 10.7 cm). Figure 2.4(b) shows the results of using the lower stratosphere (50–150 hPa) temperature from channel 4 of the Microwave Sounding Unit (MSU) on the NOAA series of polar-orbiting meteorological satellites (Randel and Cobb, 1994). Figure 2.4(c) shows the results of using 500 hPa data from the National Meteorological Center (NMC) analyses.

From Figure 2.4 it can be seen that, for most of the data, the Athens and Mediterranean values are very close to one another (see also Section 3.2). They also generally follow the 40°N zonal mean derived from TOMS data. Thus, taking the effects of dynamical perturbations on TOC trends into account, it seems plausible to use tropospheric or stratospheric temperature as an index of dynamical variability. The use of temperature has an additional advantage, since the effects of the QBO and to some extent the F10.7 (or UV radiation) are implicitly included in temperature changes (Chandra *et al.*, 1996).

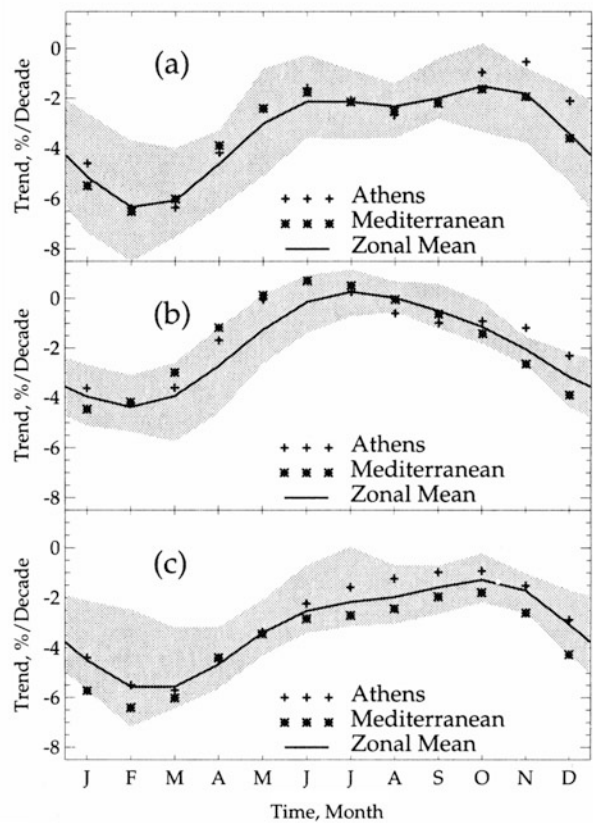


**Figure 2.4.** Monthly trends in total ozone in the Mediterranean region and at Athens compared with the trends derived from zonally averaged data. Also shown in this figure is the range of variability in seasonal trends over the latitude circle centered at 40°N (shaded). The regression models in the three panels contain (a) QBO and solar cycle terms, (b) lower-stratospheric temperature (MSU) term, and (c) the NMC 500 hPa temperature (Chandra *et al.*, 1996).

Inspection of [Figure 2.4](#) suggests a significant difference in both zonal and regional trends according to season even though relative differences between the Mediterranean and the zonal mean trend do not vary significantly. In general, TOC trends are reduced by 1 to 3%, as a result of using the MSU temperature as a proxy for dynamical variability. This is mainly due to negative trends in lower-stratospheric temperature, which vary from  $-1.5$  to  $-2$  K per decade during winter (Chandra and Stolarski, 1991; Randel and Cobb, 1994). Similar analysis using the National Meteorological Center (NMC) temperature results in a smaller change in TOC trends of 1% or less. This is probably due to the positive trend of about 0.4 to 0.8 K during the same period in the 500 hPa temperature time series.

The afore-mentioned phase change in the trend of temperature from the troposphere to the stratosphere is consistent with the changes in stationary wave patterns suggested by Hood and Zhou (1998).

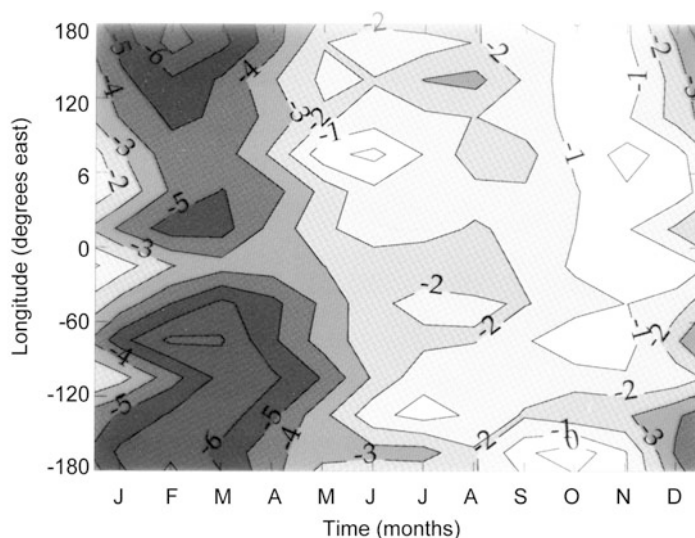


**Figure 2.5.** A cross-section of monthly trends in column ozone over the latitude belt 35°N–45°N derived from the 13 years of Nimbus-7 TOMS measurements (version 7). The trend values are given in % per decade. Negative and positive longitudes correspond to west and east longitudes, respectively (Varotsos *et al.*, 1997a).

#### 2.4.2 Longitudinal variation of TOC

Re-examination of the influence of interannual variability on satellite-derived trends in total ozone during winter and spring confirms that dynamical perturbations in the atmosphere cause large longitudinal spread in total ozone trends at mid-latitudes (Varotsos and Kondratyev, 1998a).

Figure 2.5 is a cross-section of TOC trends (% per decade) as a function of the month of the year and longitude from 180°W to 180°E in the region covering the latitude band from 35°N to 45°N (centered at 40°N). This figure shows negative trends in all seasons over the entire latitude belt centered at 40°N and is generally consistent with the pattern discussed by Chandra *et al.* (1996). The trends vary from –1 to –2% per decade during summer to –2 to –6% per decade during winter. The  $2\sigma$  uncertainties associated with these trends are in the range of 2 to 3% in summer and 3 to 6% in winter. Chandra *et al.* (1996), using the same analysis but with version 6 TOMS data, found that the trends vary from –2 to –3% per decade during summer to –3 to –9% per decade during winter.

### 2.5 SATELLITE INSTRUMENTATION FOR OVP OBSERVATIONS

Satellite-based techniques and instruments for OVP observations are presented in this section. Note that the satellite-based solar occultation technique and satellite-based nadir measurements have important advantages over ground-based measure-

ments, because they provide near-global distributions, as opposed to point measurements from ground-based *in situ* techniques. It is self-calibrating because unattenuated sunlight is measured during each event allowing data to be normalized to extra-atmospheric values. The longer absorption path in the limb geometry provides higher sensitivity than that from nadir-looking geometry. Moreover, higher vertical resolution is inherent in this technique because most of the absorption occurs at the tangent altitude. Finally, this technique simplifies data interpretation because the Sun is used as a constant background source.

Note that the first instrument used to measure ozone in the 55–85 km region was a UV spectrometer and polarimeter onboard the Solar Maximum Mission spacecraft launched in February 1980. This used the technique of solar occultation in the UV region by the Earth's limb. The first attempts at satellite occultation sounding were conducted from Soviet manned spacecraft (Kondratyev, 1972, 1998b; Kondratyev *et al.*, 1996). The Russian Ozone and Aerosol Fine Structure (OZAFS) experiment obtained a few ozone profiles from satellite occultation sounding aboard the Soviet Salyut-7 orbiting station in 1965.

### 2.5.1 Direct-absorption measuring instruments

A few instruments use the Beer–Lambert–Bouguer law to determine ozone concentration by directly measuring the absorption features of ozone either within a path defined by the instrument or by using an extraterrestrial source (i.e., the Sun). The main advantage of direct absorption measuring instruments is that in the data-processing algorithm only a few assumptions have to be made regarding quantities that are not directly measurable. However, their main disadvantage is the uncertainty of the absorption cross-section and also the limited signal-to-noise ratio at the extreme measurement range.

In general, direct absorption measuring instruments are divided into two groups according to the source of the radiation they use. Those instruments that rely on an external radiation source (i.e., the Sun or the Moon) are called “passive” instruments (i.e., optical ozonesondes, IR spectrometers, and the laser heterodyne spectrometer). Passive instruments usually measure an average molecular density along the atmospheric path (observing at sunrise or sunset from above the atmosphere or descending through the atmosphere).

Instruments with their own radiation sources are called “active” instruments and include the source, the atmospheric path length, the collector, the aperture, the spectral analyzer, the detector, the signal chain, the data storage unit, and the instrument controller (i.e., DIAL, UV photometer).

#### 2.5.1.1 Stratospheric Aerosol and Gas Experiment (SAGE)

The SAGE instruments are satelliteborne multichannel radiometers that measure gas extinction profiles using solar occultation. SAGE I was launched aboard the dedicated Applications Explorer Mission-2 (AEM-2) in February 1979 and operated for 34 months until November 1981, when the spacecraft's electrical system failed.



SAGE II was launched on the Earth Radiation Budget Satellite (ERBS) in October 1984 and globally monitored the vertical distribution of stratospheric aerosols, ozone, water vapor, and nitrogen dioxide, by measuring the extinction of solar radiation through the atmosphere during ERBS solar occultations (Mauldin *et al.*, 1985, 1986). Both SAGE I and SAGE II are in approximately 600 km circular orbits with inclination angles of 56 and 57°, respectively. They measure the absorption of sunlight by ozone with four channels (SAGE I), at 0.385, 0.45, 0.6 and 1.0  $\mu\text{m}$  wavelengths at spacecraft sunrise and sunset (solar occultation geometry). The 0.6  $\mu\text{m}$  channel is used to measure stratospheric ozone by using the Chappuis band. The 0.45  $\mu\text{m}$  channel is used to measure the concentration of stratospheric  $\text{NO}_2$ , and the other two channels are used to determine aerosol optical depth. Vertical resolution is approximately 1 km for altitudes above 10 km. SAGE II is a seven-channel instrument and—in addition to ozone,  $\text{NO}_2$ , and aerosols—it measures water vapor concentrations. It makes measurements up to 65 km as against 55 km for SAGE I. The extra channels enable better corrections for aerosols to be made. SAGE III is an improved version with higher spectral resolution, greater spectral wavelength coverage, and a lunar occultation capability, which allows for a broader range of latitudes (than that of solar occultation) and for the measurements of  $\text{NO}_3$  and  $\text{ClO}_2$ . It relies upon the flight-proven designs used in the Stratospheric Aerosol Measurement (SAM I) and the first and second SAGE instruments. In SAGE III (for the Earth Observing System Program) the filters are replaced by a spectrometer, a diode array is used for detecting radiation in the various wavelength regions, and the spectral range is extended to 1.55  $\mu\text{m}$  for observation of aerosols with larger particles and aerosols near the Earth's surface. This configuration enables SAGE III to make multiple measurements of absorption features of target gaseous species and multiwavelength measurements of broadband extinction by aerosols from the middle troposphere through the stratosphere. By making these measurements in the correct color region, SAGE III produced accurate profiles of ozone or water vapor (NASA). One SAGE-III instrument was launched on board the Russian spacecraft METEOR 3M in 1998 (polar Sun-synchronous orbit), and another was launched from Baikonur, Russia, on December 10, 2001 for installation on the International Space Station (51.5° inclination orbit).

Regarding precision and accuracy, the major uncertainty in the ozone concentrations measured by either SAGE I or SAGE II is Chappuis band ozone absorption cross-sections and their temperature dependences, which are estimated to give a 6% uncertainty. The measurement precision of SAGE II is 4–7% in the 15–52 km altitude range, becoming 20% at 60 km and 50% at 10 km. When statistical and systematic uncertainties are combined, accuracy is better than 10% for heights between 15 and 52 km. Figure 2.6 shows the differences between ozone measurements made by various different systems and by SAGE-II (WMO, 1999)..

### 2.5.1.2 Atmospheric Trace Molecule Spectroscopy (ATMOS)

The first chemically comprehensive set of space-based measurements was made by the ATMOS instrument, an infrared occultation interferometer. This instrument

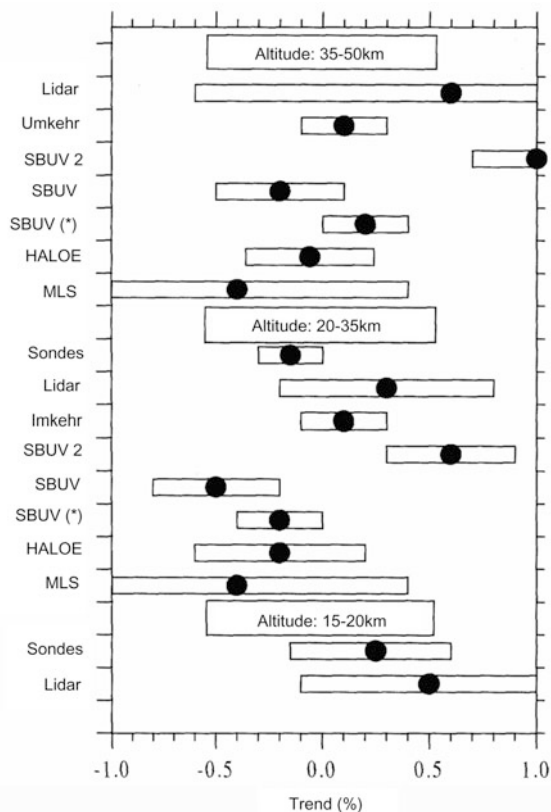


**Figure 2.6.** Trends of differences (i.e., drifts) between ozone measurements made by various ozone-profiling instruments and SAGE-II, in % per year  $[(\text{Sounding} - \text{SAGE-II})/\text{SAGE II}]$ . The trends of ozonesondes, lidar, and Umkehr differences are presented as averages for eight northern mid-latitude sounding stations. The trends of satellite differences are presented as global means. Average differences are indicated by dots, and bars represent the 99% confidence interval of drift estimation. The entries for SBUV are for SBUV/SAGE II comparison; the entries for SBUV\* are for SBUV/combined SAGE I and SAGE II comparison (WMO, 1999).

uses a Fast Fourier Transform (FFT) interferometer, which operates in the near and mid-infrared region of the spectrum to detect many molecular constituents in the upper atmosphere and to measure their vertical and horizontal distributions. It was first flown aboard the Shuttle *Challenger* (as a part of *Spacelab 3*) in April–May 1985 and measured solar radiation at sunsets and sunrises (as seen from the orbiter). Twenty occultations were recorded from this experiment and these produced simultaneous concentration profiles for a large number of minor upper-atmosphere species, several of which had not previously been observed. Simultaneity of observations is a very important aspect in the study of the highly interactive nature of photochemical processes. Subsequent flights of the ATMOS instrument (March 1992, April 1993, November 1994) extended ATMOS coverage to the tropics and

high latitudes and were used for trend determination by comparison of the mid-1985 and late-1994 observations (Grant, 1989).

### 2.5.1.3 Polar Ozone and Aerosol Monitor (POAM)

The POAM II instrument is a satelliteborne multichannel radiometer similar to SAGE II. It was carried onboard the Système Pour l'Observation de la Terre (SPOT-3) satellite in an orbit similar to that of the SAM-II sensor on the Nimbus-7 satellite (i.e., a Sun-synchronous  $98^\circ$  inclination, 833 km orbit with a 10:30 LT equatorial crossing time). In normal operation, it provided for Southern Hemisphere observations much closer to the South Pole, extending to  $88^\circ\text{S}$  at the vernal equinox from October 15, 1993 until November 14, 1996. It is a solar occultation instrument with nine narrowband channels between 352 and 1,060 nm that retrieve stratospheric ozone, aerosol extinction,  $\text{NO}_2$ , and water vapor (Glaccum *et al.*, 1996). Its ozone profiles were used to study the breakup of the 1993 Antarctic polar vortex (Bevilacqua *et al.*, 1995), polar vortex dynamics during the 1994 and 1995 northern winters (Randall *et al.*, 1995), and polar mesospheric clouds in the Southern Hemisphere (Debrestian *et al.*, 1997; Fromm *et al.*, 1997).

One POAM instrument called the "Orbiting Ozone and Aerosol Monitor" (OOAM) flew on a  $45^\circ$  inclination orbit in the summer of 1997. Another POAM III instrument flew in early 1998 on the French SPOT-4 satellite in a polar Sun-synchronous orbit observing ozone at the wavelength of  $0.603\text{ }\mu\text{m}$ .

### 2.5.1.4 Halogen Occultation Experiment (HALOE)

This instrument (Figure 2.7) was flown on the Upper Atmosphere Research Satellite (UARS) covering two longitude sweeps each day (15 profiles each): one at the latitude of sunsets and one at the latitude of sunrises. Each sunrise or sunset observation is separated by 1.6 hr and  $24^\circ$  longitude. It has eight infrared channels (from 2.45 to  $10.01\text{ }\mu\text{m}$ ): four are broadband ( $60\text{--}120\text{ cm}^{-1}$ ) filter radiometer channels for  $\text{CO}_2$ ,  $\text{H}_2\text{O}$ ,  $\text{O}_3$ , and  $\text{NO}_2$  and four are gas filter correlation radiometer channels for HF, HCl,  $\text{CH}_4$ , and NO.

The HALOE instrument uses the principle of the satellite solar occultation technique, and the measurement principle is based on both gas filter correlation radiometry and broadband filter radiometry (Figure 2.7). In the first technique incoming radiation is split into different channels for each species and passed through a narrowband filter; it is then further split into two paths for each species. One path includes a cell containing the gas to be measured.

As the atmosphere passes in front of the Sun, the path containing the cell will see little change in absorption, because the appropriate portion of the Sun's spectrum is already absorbed by the gas in the cell. The conventional broadband technique is described in other sections describing other instruments (e.g., LIMS in Section 2.5.3.1). The vertical resolution for the retrievals of aerosol,  $\text{NO}_2$ ,  $\text{H}_2\text{O}$ , and  $\text{O}_3$  is 2 km. The accuracy for ozone-mixing ratios is estimated to be 10–15% in the mid-stratosphere, with a decrease in accuracy above and below this region (Grant, 1989).

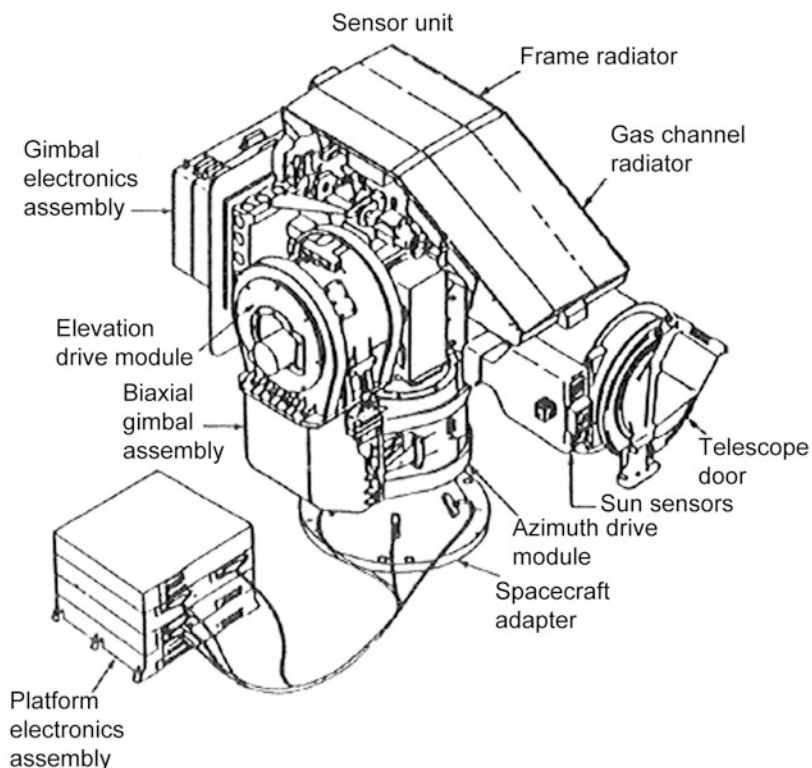


**Figure 2.7.** HALOE instrument (NASA, 1986).

Data obtained from the Halogen Occultation Experiment (HALOE) on board the Upper Atmospheric Research Satellite (UARS) during the period 1992–2004 have been analyzed by Fadnavis and Beig (2010) to study the effect of the 11-year solar cycle using a multifunctional regression model. The effects on ozone were analyzed over the 0–30°N and 0–30°S belts. The solar effect on ozone was found to be significant in most of the stratosphere:  $2 \pm 1.1$  to  $4 \pm 1.6\%$ /100 sfu (solar flux unit). It is negligible in the lower mesosphere whereas it is of the order of 5%/100 sfu in the upper mesosphere. These observed results were in reasonable agreement with model simulations.

Stellar occultations obtained by the Solar–Stellar Irradiance Comparison Experiment (SOLSTICE) on board UARS are also used to study the ozone concentration in the mesosphere between 55 and 85 km (de Toma *et al.*, 1998).

#### **2.5.1.5 SunPhotometer Earth Atmosphere Measurement (SPEAM)**

This Canadian instrument was flown on the U.S. Space Shuttle *Challenger* in October 1984 and provided observations at 315 and 324 nm at 63.34°S, 81.96°E, from which OVPs are inferred. Observations started several minutes before the

occultation time. The instrument was manually pointed at the Sun through the quartz window, and this was maintained until the occultation was over. The small size of the instrument, and the fact that it can be returned to the laboratory for calibration between flights, make this technique very useful. It was also flown on the Space Shuttle in 1992 making measurements of  $O_3$ ,  $NO_3$ , and  $NO_2$ . It was actually a dual-wavelength interference filter sunphotometer, similar to the commercial single-channel device, formerly used in the Canadian solar radiation network. The flight version of it (STS 41-G) differs from its conventional ground-based version in that it can observe simultaneously at two different wavelengths (McElroy *et al.*, 1991). SPEAM made measurements as a part of a Canadian payload aboard two Space Shuttle flights: STS-41G in October 1984 and STS-52 in October 1992.

### 2.5.1.6 The Atmospheric Chemistry Experiment (ACE)

One of the newest satellites for solar occultation studies is the Atmospheric Chemistry Experiment (ACE) developed for remote sensing of the Earth's atmosphere. This Canadian-led satellite mission, also known as SCISAT-1, was launched on August 12, 2003. There are two instruments on board the spacecraft that provide vertical profiles of ozone and a range of trace gas constituents, as well as temperature and atmospheric extinction due to aerosols. The ACE Fourier Transform Spectrometer (ACE-FTS) measures in the infrared (IR) region of the spectrum and the Measurement of Aerosol Extinction in the Stratosphere and Troposphere Retrieved by Occultation (ACE-MAESTRO) operates in the UV/visible/near-IR.

The main objective of the ACE mission was to understand the global-scale chemical and dynamical processes that govern the abundance of ozone from the upper troposphere to the lower mesosphere, with an emphasis on chemistry and dynamics in the Arctic. SCISAT, the platform carrying the ACE-FTS and ACE-MAESTRO, is in a circular low-Earth orbit, with a  $74^\circ$  inclination and an altitude of 650 km. From this orbit, the instruments measure up to 15 sunrise (hereinafter SR) and 15 sunset (hereinafter SS) occultations each day. Global coverage of the tropical, mid-latitude, and polar regions (with the highest sampling in the Arctic and Antarctica) is achieved over the course of one year and the ACE measurement latitude pattern repeats each year.

The primary instrument for the ACE mission, the ACE-FTS (Figure 2.8), is a successor to the Atmospheric Trace MOlecule Spectroscopy (ATMOS) experiment, an infrared FTS that operated during four flights on the Space Shuttle (in 1985, 1992, 1993, and 1994). ACE-FTS measures high-resolution ( $0.02\text{ cm}^{-1}$ ) atmospheric spectra between  $750$  and  $4,400\text{ cm}^{-1}$  ( $2.2\text{--}13\text{ }\mu\text{m}$ ). This sensor uses the solar occultation technique to determine the profiles of atmospheric trace gases, temperature pressure, and aerosols. A feedback-controlled pointing mirror is used to target the center of the Sun and track it during the measurements. Typical signal-to-noise ratios are more than 300 from  $900$  to  $3,700\text{ cm}^{-1}$ . From the 650 km ACE orbit, the instrument's field of view ( $1.25\text{ mrad}$ ) corresponds to a maximum vertical resolution of  $3\text{--}4\text{ km}$ . The vertical spacing between consecutive second ACE-FTS measurements depends on the satellite's orbital geometry during occultation and can



**Figure 2.8.** The ACE-FTS instrument (interferometer side) ([http://www.ace.uwaterloo.ca/instruments\\_acefts.html](http://www.ace.uwaterloo.ca/instruments_acefts.html)).

vary from 1.5 to 6 km. The altitude coverage of the 20 measurements extends from the cloud tops to 100–150 km.

The Measurement of Aerosol Extinction in the Stratosphere and Troposphere Retrieved by Occultation (ACE-MAESTRO) is a dual-grating diode array spectrophotometer that extends the wavelength range of ACE measurements into the near-IR to UV spectral region (Figure 2.9). It records over a nominal range of 400–1,010 nm with a spectral resolution of 1.5–2 nm for its solar occultation measurements. The forerunner of the ACE-MAESTRO is the Sun Photo Spectrometer instrument which was used extensively by Environment Canada as part of the NASA ER-2 stratospheric chemistry research program. ACE-MAESTRO uses the same Sun-tracking mirror as the ACE-FTS, receiving 7% of the beam collected by the mirror. The ACE-MAESTRO instrument's vertical field of view is 1 km at the limb (Figure 2.9). Observation tangent altitudes range from the surface to 100 km with a vertical resolution estimated at better than 1.7 km.

The processing of ACE-MAESTRO version 1.2 occultation data is done in two stages and is described by McElroy *et al.* (2007). In summary, the raw data are



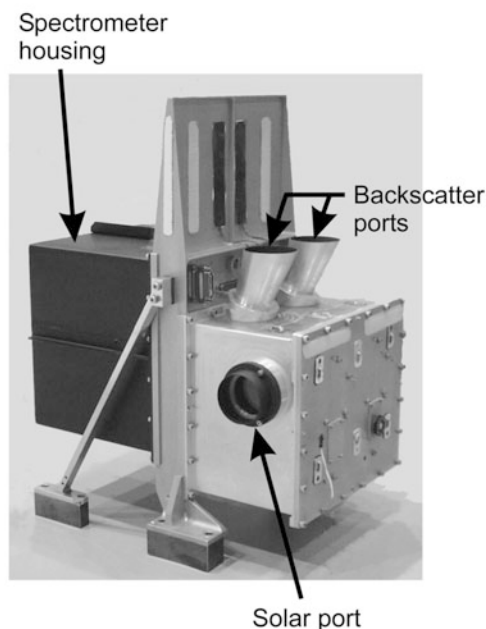


**Figure 2.9.** Photograph of the MAESTRO instrument, showing occultation (solar) and backscatter viewing ports (McElroy *et al.*, 2007).

converted to wavelength-calibrated spectra, corrected for stray light, dark current, and other instrument parameters in the first step. The corrected spectra are then analyzed by a non-linear least squares spectral-fitting code to calculate slant path column densities for each spectrum, from which the vertical profiles of  $\text{O}_3$  and  $\text{NO}_2$  volume-mixing ratios are subsequently derived. The retrieval algorithm does not require any *a priori* information or other constraints. The inversion routine uses the pressure and temperature profiles and tangent heights from the ACE-FTS data analysis to fix the tangent heights for ACE-MAESTRO. Vertical profiles for the trace gases are determined by adjusting an initial guess (high vertical resolution model simulation) using a non-linear Chahine relaxation inversion algorithm. The final profiles are provided both on the tangent grid and interpolated onto a 0.5 km spacing vertical grid (Dupuy *et al.*, 2009).

#### 2.5.1.7 Upcoming ESA Mission

PREMIER (PRocess Exploration through Measurements of Infrared and millimeter wave Emitted Radiation) is one of the three candidate Earth Explorer mission concepts to progress to the next phase of consolidation. Following a further down-selection, this will lead to ESA's seventh Earth Explorer mission envisaged to be launched around 2016.

The PREMIER candidate mission aims to quantify the processes that control the composition of the mid to upper troposphere and lower stratosphere—which



equates to 5–25 km above the surface of the Earth. This region of the atmosphere is particularly important for climate studies because it is where the atmosphere cools to space and where it is most sensitive to changes in the distribution of radiative gases and clouds. Through the transport of water vapor, ozone, methane, clouds, and aerosols, this region is host to numerous important interactions between the composition of the atmosphere and climate.

PREMIER will address these issues by measuring temperature, water vapor, and a large number of trace gases such as ozone and methane at high spatial resolution. The proposed mission concept employs two innovative instruments: an infrared-imaging spectrometer and the first millimeter wave sounder optimized for the upper troposphere. These instruments are based on proven heritage used on earlier missions such as the millimeter wave radiometer on the Swedish Odin satellite, which is now an ESA Third Party mission, and the MIPAS (Michelson Interferometer for Passive Atmospheric Sounding) instrument on ENVISAT.

The payload complement of PREMIER consists of two instruments observing the limb of the Earth: (a) the Millimeter Wave Limb Sounder (MWLS) and (b) the Infra-Red Limb Sounder/Cloud Imager (IRLS/IRCI).

The Millimeter Wave Limb Sounder (MWLS) concept description is based on the STREAMR instrument concept being developed by the Swedish Space Corporation within the framework of the dedicated Swedish National Program.

The STREAMR instrument is designed to provide spatially well-resolved (1–2 km vertically and 50 km horizontally) information on the distribution of Upper Troposphere/Lower Stratosphere (UT/LS) key constituents such as water vapor, ozone, and carbon monoxide on a global scale using bands in the 310–360 GHz spectral region. The STREAMR measurement concept is based on tomographic multibeam limb sounding in the orbital plane using Schottky diode heterodyne detectors. The instrument observes the limb at 14 tangent altitudes simultaneously with a staring view concept.

An offset antenna system receives thermal radiation from the atmospheric limb. Additional optical elements fold the path and refocus the beams on the focal plane. Calibration devices can be viewed by rotating a switch mirror close to the secondary aperture stop. A second rotating mirror selects the calibration source from one of two cold-sky views: a temperature-controlled warm load or a sideband filter to calibrate the sideband ratios.

Individual mirror–horn combinations couple the signals to the waveguides of the 14 sub-harmonically pumped Schottky mixers integrated with low-noise amplifiers. The down-converted signals in the 9 to 21 GHz spectral region are distributed after amplification to a set of autocorrelation spectrometers and divided into six separate units to simplify thermal control.

The Infra-Red Limb Sounder and Cloud Imager (IRLS/IRCI) instrument is a Fourier transform spectrometer combining the functions of spectrometry and imagery. The IRLS provides two mutually exclusive measurement modes: the atmospheric Chemistry Mode, featuring the highest spectral resolution to observe minor trace gases, and the atmospheric Dynamics Mode, providing a higher spatial resolution in order to resolve finer atmospheric structures. The IRCI must work

continuously, acquiring images at a high spatial resolution in the same spectral ranges as the IRLS but with a reduced spectral resolution ( $10\text{--}20\text{ cm}^{-1}$ ).

The spectral range of the IRLS covers two bands: band A ( $770\text{--}980\text{ cm}^{-1}$  or  $10.2\text{--}13\text{ }\mu\text{m}$ ) and band B ( $1070\text{--}1650\text{ cm}^{-1}$  or  $6.0\text{--}9.4\text{ }\mu\text{m}$ ). The spectral resolution is  $0.2\text{ cm}^{-1}$  and  $1.25\text{ cm}^{-1}$  in the chemistry and dynamic modes, respectively.

The IRLS measures limb radiance at vertical spatial-sampling intervals of 2 km and 0.5 km in the chemistry and dynamic modes, respectively. Radiance from the limb enters the instrument via a pointing mirror, which is also used to view cold space, and a flat or cavity blackbody for calibration. After beam size adaption in the afocal telescope, a Michelson interferometer produces interferograms, which are acquired by two detector arrays after band splitting by a dichroic filter. A laser metrology system, using a diode laser or a Nd:YAG laser, monitors the path difference between the two arms. The detectors are cooled to 55 K with Stirling cycle or pulsed tube coolers, with the possibility of operating the band B detectors at a slightly higher temperature (ESA, 2008).

## 2.5.2 Scattering-measuring instruments

### 2.5.2.1 Shuttle Ozone Limb Sounding Experiment (SOLSE)

The SOLSE is an ozone-measuring payload which was flown on board the Space Shuttle in the autumn of 1997 and included two UV instruments (Section 2.5.2.2). One was the Shuttle Ozone Limb Sounding Experiment (SOLSE). This is a spectrometer that uses UV wavelengths consisting of a two-dimensional detector (altitude wavelength). It measures ozone concentration in the stratosphere and upper troposphere (Hilsenrath *et al.*, 1991).

### 2.5.2.2 Limb Ozone Retrieval Experiment (LORE)

LORE and SOLSE were the two UV instruments of the ozone-measuring payload flown aboard the Space Shuttle in the autumn of 1997. LORE is a multiwavelength version of the Rayleigh Scattering Attitude Sensor (RSAS), a single-channel (355 nm) instrument that flew with SSBUV on STS-72 in January 1996. It uses optical filters and covers the UV, visible, and infrared channels. It obtains ozone profiles as low as the 10–15 km altitude range (Hilsenrath *et al.*, 1991).

### 2.5.2.3 Solar Mesospheric Explorer-Ultraviolet Spectrometer (SME-UVS)

The ultraviolet spectrometer (UVS) on the Solar Mesosphere Explorer (SME) satellite is designed to measure the ozone density of the mesosphere in the 1.0–0.1 hPa (48–70 km) region at sunlit latitudes. To achieve this, the instrument measures altitude profiles of Rayleigh-scattered solar photons in the 200–340 nm spectral region.

This instrument has an off-axis parabolic telescope, an Ebert–Fastie grating spectrometer, and a pair of photomultiplier tubes. The spectrometer is used at a

pair of fixed wavelengths separated by approximately 30 nm (265.0 and 296.4 nm) and operates with a spectral resolution of 1.5 nm. The spacecraft rotates at 5 rpm and observes the Earth's limb, leading and trailing the SME ground track. It measures the altitude profiles of Rayleigh-scattered UV. Random errors vary from 3.4% at a height of 48 km to 10.2% at 68 km. Temperature and pressure errors vary from 4.5% at 48 km to 10.1% at 68 km. The SME-UVS provided a number of ozone density datasets in the measured ozone concentration, which help to explain ozone photochemistry (Grant, 1989). The Solar Maximum Mission (SMM) spacecraft carried a high-resolution ultraviolet spectrometer polarimeter (UVSP), employed since 1980 to measure the ozone profile by the technique of solar occultation (Aikin, 1989).

#### 2.5.2.4 *Solar Mesosphere Explorer (SME)-Near-IR Spectrometer*

This instrument uses an off-axis parabolic mirror and an Ebert–Fastie spectrometer. There are two channels with a resolution of 12 nm and a separation of 0.6  $\mu\text{m}$ . The 1.27  $\mu\text{m}$  channel is used for emission measurements and the 1.87  $\mu\text{m}$  channel is used for reference purposes (i.e., to correct data for radiances that are due to oxygen emission). Random error sources for ozone density include temperature (3% at 50 km, 1% at 90 km); systematic errors include calibration errors (10% in the laboratory before launch and 20% after launch).

The SME Near-Infrared Spectrometer has generated a number of datasets on spatiotemporal variations in ozone concentration since its launch in October 1981. A similar instrument was developed in Japan, the Infrared Air-glow (IRA), and flew on board the EXOS-C satellite (Ogawa *et al.*, 1989).

#### 2.5.2.5 *SCanning Imaging Absorption Spectrometer for Atmospheric Chartography (SCIAMACHY)*

This is a multichannel spectrometer measuring radiation in the spectral range 240–1,750 nm at relatively high resolution (0.2 nm–0.5 nm) on board the European satellite ENVISAT-1, launched in 1999. This instrument was designed to measure the column and profile distribution of a number of gases, including high horizontal resolution measurements of ozone. It is a combination of two spectrometers also operating in the UV/visible/near-infrared part of the spectrum to observe transmitted, reflected, and scattered light. It provides measurements from nadir (scattered and reflected solar photons), limb (scattered and reflected solar photons), occultation (transmitted solar or lunar photons), and solar reference (extraterrestrial solar photons), achieving global coverage within three days.

From the limb measurements, the stratospheric profiles of pressure, temperature, and several trace gases ( $\text{O}_3$ ,  $\text{O}_2$ ,  $\text{O}_4$ ,  $\text{NO}$ ,  $\text{NO}_2$ ,  $\text{NO}_3$ ,  $\text{N}_2\text{O}$ ,  $\text{CO}$ ,  $\text{CO}_2$ ,  $\text{CH}_4$ ,  $\text{H}_2\text{O}$ ,  $\text{BrO}$ ,  $\text{ClO}$ ,  $\text{OCIO}$ ,  $\text{HCHO}$ ,  $\text{SO}_2$ , and aerosol) can be retrieved (Kramer, 2002; Rozanov *et al.*, 1997).

### 2.5.2.6 FY-3 Total Ozone Unit (TOU)

FY-3 satellites are Chinese second-generation polar orbit meteorological satellites. The Total Ozone Unit (TOU) is one of the main payloads on FY-3 satellites and the first instrument for daily global coverage of total ozone monitoring in China. The main purpose of TOU is to measure the Earth's backscatter ultraviolet radiation for retrieving a daily global map of atmospheric ozone. TOU will provide the important parameters for environmental monitoring, climate forecasting, and global climate change research.

TOU is an instrument used to measure incident solar radiation and backscattered ultraviolet radiance such that total ozone can be retrieved. Considering the characteristics of the atmospheric ozone profile, the measuring wavelength should be selected so that its effective scattering layer is situated in the troposphere in order to ensure the accuracy of measuring total ozone from the satellite.

The effective scattering layer for 302.5 nm is situated above the height of the ozone maximum and that for the 307.5 nm has two effective scattering layers. Therefore, the shortest wavelength for measuring total ozone should be longer than 308 nm.

Using the single-wavelength method makes it difficult to obtain total ozone precisely. Therefore, a wavelength pair method is used to eliminate the effects of atmospheric molecular scattering and aerosol scattering. In this method, a non-ozone-absorbing wavelength is used to obtain the reflectivity of underlying surfaces and the heights of cloud tops (Wang *et al.*, 2009).

### 2.5.3 Emission-measuring instruments

A few instruments measure ozone in emissions, observing features from the near-IR to millimeter wavelengths. These instruments observe the Earth's limb from a space-borne platform, and some are used in nadir-viewing directions (Grant, 1989; Kramer, 2002). The signals in emissions are generally weaker than those in absorption and, therefore, the instruments are generally cooled, except the millimeter wave ones (they can observe in very narrow spectral regions using heterodyne detection techniques).

#### 2.5.3.1 Limb Infrared Monitor of the Stratosphere (LIMS)

The first space-based measurements of stratospheric trace constituents (besides ozone) were made from the Limb Infrared Monitor of the Stratosphere (LIMS) and the Stratosphere and Mesosphere Sounder (SAMS) on board Nimbus-7.

LIMS is a cryogenically cooled limb-scanning infrared filter radiometer, launched on Nimbus-7 in 1978 with a lifetime of 7 months. It was developed from the earlier Limb Radiance Inversion Radiometer (LRIR) with a limited number of channels. It has six channels (centered between 6.2 and 15.0  $\mu\text{m}$ ) that permit observation of emissions by  $\text{CO}_2$ ,  $\text{HNO}_3$ ,  $\text{O}_3$ ,  $\text{H}_2\text{O}$ , and  $\text{NO}_2$ .

Two channels near 15  $\mu\text{m}$  can be used to retrieve vertical temperature profiles. The other channels are used for molecular species measurements. Ozone, for

example, is observed in the  $926\text{--}1,141\text{ cm}^{-1}$  spectral region, with a vertical field of view of 1.8 km and a horizontal field of view of 18 km from 15 to 64 km altitude. Because of its geometry, this technique has an inherently high vertical resolution and can sound at high altitudes. The instrument scans from above the atmosphere to below the Earth's horizon and back every 24 s. The precision of this instrument was found to vary from 2–4% at 30 hPa to 1% at 0.4 hPa. Absolute accuracy was about 10%. Many experiments provided data about the distribution and variability of temperature and several minor constituents ( $\text{O}_3$ ,  $\text{H}_2\text{O}$ ,  $\text{HNO}_3$ , and  $\text{NO}_2$ ) over the latitude range from  $84^\circ\text{N}$  to  $64^\circ\text{S}$ . Some data on ozone and aerosol profiles in the stratosphere were also obtained by the Aerosol Limb Absorption (ALA) instrument which flew on board the Japanese Ohzora satellite, launched in February 1984. ALA was a two-channel sunphotometer (6,500, 1,000 nm) that used the solar occultation technique. Another occultation instrument, the Limb Atmospheric Infrared Spectrometer (LAS) also flew aboard Ohzora (Ogawa *et al.*, 1989).

### 2.5.3.2 Solar Mesosphere Explorer Near-Infrared Spectrometer (IRS/SME)

The near-infrared spectrometer (NIRS) on board the SME satellite was designed to carry out ozone measurements between 50 and 90 km over most latitudes at 3:00 PM local time. The instrument measures emission from  $\text{O}_2$  ( $^1\Delta g$ ) at  $1.27\text{ }\mu\text{m}$  that is primarily due to the photodissociation of ozone. Vertical resolution is better than 3.5 km. Note that at the time of the El Chichón eruption in 1982, there was no SAGE instrument operating and data about the eruption were obtained from SME (Grant, 1989).

### 2.5.3.3 Michelson Interferometer (IRIS, MIPAS)

This instrument (IRIS-D) was designed to record the infrared emission spectrum of the Earth and its atmosphere between  $400\text{ cm}^{-1}$  and  $1,600\text{ cm}^{-1}$  in order to provide the vertical profiles of temperature, humidity, and ozone concentration. IRIS-D launched on board Nimbus-4 is an advanced version of the IRIS-B launched on board Nimbus-3 a year earlier (on April 14, 1969). The subsequent improvement resulted in an increase in spectral resolution from  $5\text{ cm}^{-1}$  to  $2.8\text{ cm}^{-1}$ .

The MIPAS (Michelson Interferometer for Passive Atmospheric Sounding) is a middle-infrared Fourier transform spectrometer operating on board the ENVISAT platform and acquiring high-resolution spectra of atmospheric limb emission in five spectral bands within the frequency range from  $685$  to  $2,410\text{ cm}^{-1}$  ( $14.6$  to  $4.15\text{ }\mu\text{m}$ ) (Fischer *et al.*, 2007) during both daytime and nighttime with global coverage. It measures temperature, ozone, and other chemical species (especially nitrogen and chlorine-containing species) (Carlotti *et al.*, 1995; Guld *et al.*, 1994). It also measures aerosols and PSCs. In its standard observation mode, the instrument scanned 17 tangent altitudes for each limb sequence, viewing in the rearward direction along the orbit with a sampling rate of approximately 500 km along track and with a horizontal resolution across track of about 30 km. The vertical scanning grid ranges between 6 km and 68 km, with steps of 3 km from 6 to 42 km, 5 km from 42 to 52 km, and 8 km from 52 to 68 km. On a daily basis, MIPAS covered the Earth with  $5^\circ$  latitude

by  $12.5^\circ$  longitude spacing. Complete global coverage was obtained approximately every three days by 73 scans per orbit and 14.3 orbits per day scanning the latitudinal range from  $87^\circ\text{S}$  to  $89^\circ\text{N}$ . MIPAS operation was temporarily halted at the end of March 2004 because of excessive anomalies observed in the interferometric drive unit and resumed in January 2005 in a new operational mode at a reduced spectral resolution ( $0.0625\text{ cm}^{-1}$ ) and on a finer vertical grid. In addition to being flown on ENVISAT, a MIPAS instrument has also been used on a Transall C-160 aircraft (Guld *et al.*, 1994).

#### 2.5.3.4 Microwave Limb Sounder (MLS)

The MLS was originally an airborne millimeter wavelength (1.0–1.5 mm) radiometer. The present version operates in the 200–300 GHz range. Using local oscillators and filter banks (35 filters per local oscillator), brightness temperatures (day and night) at various frequencies, along emission lines from various molecular species, are measured with a vertical resolution of about 5 km. The MLS was found to have a precision of 4% and an accuracy of the order of 9%. MLS was used on board the Upper Atmospheric Research Satellite (UARS) and proposed for the Earth Observing System (EOS). It was also used in the Balloon Intercomparison Campaign (BIC). MLS has been acquiring millimeter wavelength emission measurements of the stratosphere in both hemispheres since late September 1991. Measurements are made as the instrument's field of view is vertically scanned through the atmosphere limb in a plane perpendicular to the UARS trajectory. MLS pointing geometry together with the inclination of the UARS orbit leads to measurement latitudinal coverage that extends from  $80^\circ$  on one side of the equator to  $34^\circ$  on the other (Froidevaux *et al.*, 1996).

A new MLS instrument, which was a significantly enhanced version of the UARS MLS, was flown on NASA's Aura satellite (originally known as EOS-CHEM-1) which was launched on July 15, 2004 to measure temperature, ozone, and other chemical species in the lower stratosphere and the upper troposphere. Note that, given the length of the MLS dataset, its use in studies of long-term trends and shorter term phenomena such as the Quasi-Biennial Oscillation (QBO) is becoming possible (de Toma *et al.*, 1998).

The upcoming Global Atmosphere Composition Mission (GACM) (planned launch in 2016–2020) will include a Microwave Limb Sounder along with IR and UV spectrometers. The objectives of the GACM mission are to measure ozone and related gases for intercontinental air quality ( $\text{NO}_2$ ,  $\text{SO}_2$ ,  $\text{HCHO}$ ,  $\text{CO}$ , and aerosols) and stratospheric ozone. A second-phase mission featuring an active differential absorption lidar (DIAL) system will be launched in 2022 or shortly thereafter. It will measure  $\text{O}_3$  with a vertical resolution better than 2 km and aerosols and atmospheric structure at resolutions better than 150 m.

#### 2.5.3.5 Tropospheric Emission Spectrometer (TES)

The Tropospheric Emission Spectrometer (TES) was the first satellite instrument to provide simultaneous concentrations of carbon monoxide, ozone, water vapor, and



methane throughout Earth's lower atmosphere. TES is an imaging infrared Fourier Transform Spectrometer designed especially to measure the state and composition of the troposphere (i.e., the layer of the atmosphere that extends from the Earth's surface to about 16 km in altitude). However, in principle, TES is capable of observing trace gases at any altitude and in practice its use extends from the ground up to an altitude of about 32 km so that it includes the important regions of the upper troposphere and the lower stratosphere. While the instrument can detect and measure many components of the troposphere, one of its main purposes is to study ozone. TES is flown on the Aura satellite which, as we have mentioned before, was launched on July 15, 2004. TES has both nadir and limb-viewing capability and covers the spectral range  $650\text{--}2,250\text{ cm}^{-1}$  ( $4.5\text{--}15.4\text{ }\mu\text{m}$ ) at either  $0.08\text{ cm}^{-1}$  or  $0.02\text{ cm}^{-1}$  spectral resolution.

TES has four co-aligned focal plane detector arrays of  $1 \times 16$  elements (pixels), with each array optimized for a different spectral region. Each pixel's instantaneous field of view (IFOV) is  $0.075\text{ mrad}$  high by  $0.75\text{ mrad}$  wide. At the limb, this corresponds to about 2.3 km altitude by 23 km parallel to the horizon. TES observes both in nadir view and in limb view. Limb viewing provides a much longer path through the atmosphere, and looking through a larger mass of air improves the chances of observing sparsely distributed substances that might be missed in the nadir view. Limb viewing's sideways angle also makes it easier to determine the altitudes of observed substances. But limb viewing is very susceptible to interference (only rarely does the line of sight reach the surface). Nadir viewing is less affected by clouds, but looking straight down makes it more difficult to determine altitudes. A complete description of TES is given by Beer *et al.* (2001) (see also Beer, 2006 and Schoeberl *et al.*, 2006).

Felker *et al.* (2011) described the use of TES data in combination with other information to generate a Multi-sensor Upper Tropospheric Ozone Product (MUTOP). Determination of ozone concentration in the upper troposphere (UT) layer is especially difficult without direct *in situ* measurement. However, it is well understood that UT ozone is correlated with dynamical tracers like low specific humidity and high potential vorticity. Thus the approach of Felker *et al.* (2011) was to create map view products of upper-troposphere (UT) ozone concentrations through the integration of TES ozone measurements with the two synoptic dynamical tracers of stratospheric influence: specific humidity (derived from the GOES geostationary satellite) and potential vorticity (obtained from an operational forecast model). This approach results in the spatiotemporal coverage of a geostationary platform, which is a major improvement over the much less frequent individual polar overpasses, while retaining the ability of TES to determine UT ozone concentration.

Felker *et al.* (2011) note that there are several advantages in this multisensor-derived product approach: (1) it is calculated from two operational fields (GOES specific humidity and Global Forecast System (GFS) potential vorticity (PV)), so layer average ozone can be created and used in near-real time; (2) the product provides the spatial resolution and coverage of a geostationary platform as it depicts the distribution of dynamically driven ozone in the UT; and (3) the 6-hour



temporal resolution of the imagery allows for the visualization of rapid movement of this dynamically driven ozone in the UT (see the paper by Felker *et al.*, 2011 for details on this method).

### **2.5.3.6 Cryogenic Limb Array Etalon Spectrometer (CLAES)**

This instrument measures the concentrations of members of the nitrogen and chlorine families—as well as ozone, water vapor, methane, and carbon dioxide—by observing infrared thermal emissions at wavelengths from 3.5 to 12.7  $\mu\text{m}$ . In normal operation it utilizes a telescope, a spectrometer, and a linear array of 20 detectors to perform simultaneous observations for 20 altitudes ranging from 10 to 60 km. To avoid interference from the thermal emissions of the detectors and optics the CLAES cryogenic system is used, although it limits the lifetime of the instrument. This system consists of two subsystems: a block of solid neon at  $-260^\circ\text{C}$  (cooling the detectors) and a surrounding block of solid carbon dioxide at  $-150^\circ\text{C}$  (reducing emissions from the optical system). It has been used on board the UARS research satellite (Grant, 1989).

### **2.5.3.7 Improved Stratospheric and Mesospheric Sounder (ISAMS)**

This is a filter radiometer that observes, with eight detectors, infrared molecular emissions by means of a movable off-axis reflecting telescope from 4.6 to 16.6  $\mu\text{m}$ . It utilizes a Stirling cycle refrigerator to cool its detectors to  $-195^\circ\text{C}$  and carries samples of some of the gases to be measured in cells within the instrument. Installing these cells in front of the detectors, the atmospheric radiation collected by the telescope passes through them, allowing the spectra of the gases in the cells to be matched with the spectra observed in the atmosphere. As some gases cannot be confined in cells (because of their chemical activity) ISAMS employs broadband filters to isolate portions of the spectrum and, thereby, permits measurements of the gases. The instrument flown on board UARS is an improved version of that aboard Nimbus-7 and measures the concentrations of nitrogen chemical species, as well as ozone, water vapor, methane, and carbon monoxide. CLAES and ISAMS data, through their excellent spatial and comprehensive chemical information content, have provided significant information on both chemical and transport processes in the stratosphere, including issues such as the tropical mid-latitude transport of tracers (Koutoulaki *et al.*, 1998).

### **2.5.3.8 High Resolution Dynamics Limb Scanner (HIRDLS)**

This is a multichannel limb-scanning infrared radiometer developed jointly by the U.S. and the U.K. It is carried by the EOS-CHEM platform (Figure 2.10). HIRDLS has measured temperature, ozone, and a number of trace gases with a vertical resolution of 1 km from the tropopause to the mesopause since January 23, 2005. It provides information on small-scale variability in the atmosphere for use in transport studies (Dials *et al.*, 1998).

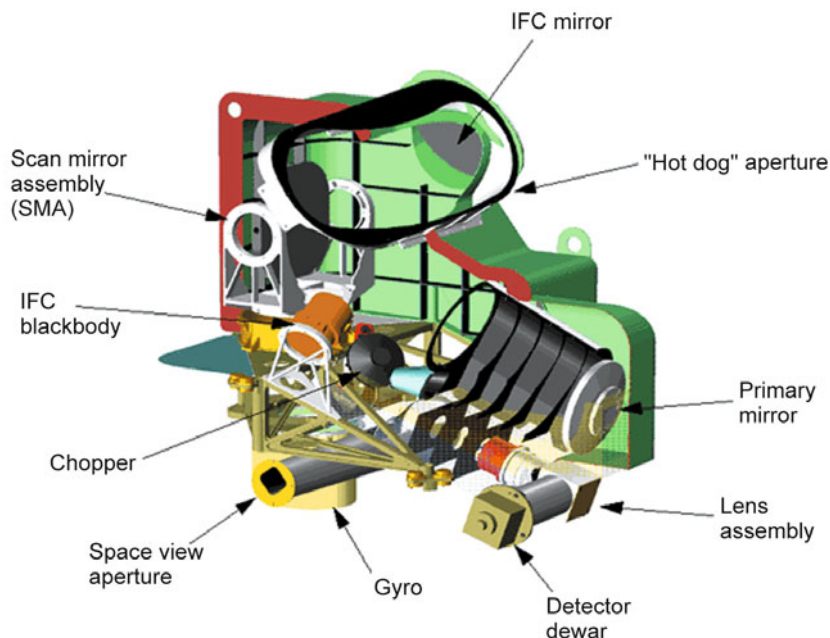


**Figure 2.10.** HIRDLS components

(<http://www.ucar.edu/communications/staffnotes/0511/hirdls.html>).

The general objectives of HIRDLS are twofold: to provide information to assess the role of the stratosphere, especially the lower stratosphere and the upper troposphere (UT/LS) in climate processes; and to observe the processes that affect the stratospheric ozone layer at a time when the concentrations of active chlorine have reached a maximum and are beginning to decrease.

#### 2.5.3.9 Cryogenic Infrared Spectrometers and Telescopes for the Atmosphere (CRISTA)

This is an infrared limb sounder designed to measure the densities of mid-atmospheric trace gases with high spatiotemporal resolution. It contains four limb-scanning liquid helium-cooled spectrometers and three telescopes that are simultaneously operated to acquire global maps of temperature and atmospheric trace gases. The telescopes (used to sense three atmospheric volumes 600 km apart) are each followed by infrared grating spectrometers; the center telescope is additionally equipped with a spectrometer for the far-infrared spectrum. A complete spectrum is measured in about 1.2 s, while a complete altitude scan is achieved in less than 1 min, providing trace gas profiles on a grid lower than 500 km × 600 km and with vertical resolution of about 2–3 km.

CRISTA was successfully used aboard the CRISTA-SPAS (Shuttle Pallet Satellite) free flyer together with ATLAS-3 (Kaye and Miller, 1996) during a

Space Shuttle mission (STS-66) in November 1994. A second flight of CRISTA and the Middle Atmosphere High Resolution Spectrographic Investigation (MAHRSI) for NO and OH observations took place in August 1997, as part of the STS-85 Space Shuttle mission. The U.S. Cryogenic Infrared Radiance Instrument for Shuttle (CIRRIS), which was designed mainly for airglow studies, was flown on board the Space Shuttle in April–May 1991 (STS-39) and relayed information on OVP and other traces.

#### **2.5.3.10 Improved Limb Atmospheric Spectrometer (ILAS)**

ILAS is an occultation instrument, getting vertical profile measurements at high northern and southern latitudes. It consists of two spectrometers, one using the infrared for trace constituent measurements and the other visible wavelengths to derive temperature and pressure profiles.

This spectrometer was developed by the Environmental Agency of Japan and installed on board the ADEOS spacecraft, which was launched on August 17, 1996. ILAS measures the vertical profiles of O<sub>3</sub>, NO<sub>2</sub>, HNO<sub>3</sub>, N<sub>2</sub>O, CH<sub>4</sub>, H<sub>2</sub>O, CFC-11, CFC-12, N<sub>2</sub>O<sub>5</sub>, and aerosols in the altitude range of 10–60 km with an altitude resolution of 1–2 km. It performs 14 measurements per day on an Arctic and Antarctic latitude circle (58–73°N, 65–90°S). ILAS O<sub>3</sub> profiles are in good agreement with ozonesonde profiles between 20 and 24 km. Higher ILAS ozone below 20 km may be attributed to the presence of aerosols, while lower ILAS O<sub>3</sub> at 24–32 km look like being due to a systematic difference between ILAS and ozonesondes, probably owing to the ILAS operational algorithm (Yushkov *et al.*, 1998). A modified version of the ILAS-II is scheduled to fly on board the Japanese ADEOS-2 satellite (see Section 2.3.3).

#### **2.5.3.11 Millimeter wave Atmospheric Sounder (MAS)**

This is a Shuttleborne limb-scanning radiometer that measures the molecular emission spectra of O<sub>3</sub>, H<sub>2</sub>O, ClO, and O<sub>2</sub> in the Earth's atmosphere, in order to provide their geographical and vertical distributions. MAS belongs to the Atmospheric Laboratory for Applications and Science (ATLAS) Shuttle payload package. It measured OVP at altitudes between 20 and 80 km over more than 90% of the Earth's surface during the three ATLAS missions (in 1992, 1993, 1994).

The MAS instrument uses a single 1 m diameter off-axis parabolic antenna (pointed toward the Earth's limb) and observes radiation along paths through the Earth's atmosphere at tangent heights from 10 to 140 km. The O<sub>3</sub> spectrum is measured with 50 RF filters, arranged in three banks (wide, intermediate, and narrow having widths of 40, 2, and 0.2 MHz, respectively).

The precision of mixing ratio results is estimated at 2–4% at altitudes of 29–62 km, increasing at both higher and lower altitudes to about 8%. Taking measurement errors into account the total uncertainty is estimated to be about 5% near the O<sub>3</sub> peak (Daehler *et al.*, 1998).

### 2.5.3.12 *Advanced Millimeter wave Atmospheric Sounder (AMAS)*

This instrument was designed as a limb-viewing, heterodyne spectrometer with two sub-millimeter receivers to measure ClO and BrO at 500 GHz and HCl at 625 GHz and receivers to measure O<sub>3</sub>, N<sub>2</sub>O, and O<sub>2</sub> in the 300 GHz region, H<sub>2</sub>O near 325 GHz and CO and HNO<sub>3</sub> close to 345 GHz. AMAS is designated for launch alongside NASA's TOMS on the Russian Meteor-3M/2 and will monitor global distributions of important constituents in the stratosphere and upper troposphere (Reburn *et al.*, 1998). The European Space Agency is investigating several scenarios for future satelliteborne limb sounders in the millimeter and sub-millimeter spectral range. For instance, MASTER is planned to be an instrument in the millimeter range focusing on the upper troposphere and on exchange processes between the troposphere and the stratosphere tracking CO, H<sub>2</sub>O, O<sub>2</sub>, SO<sub>2</sub>, N<sub>2</sub>O, and HNO<sub>3</sub> in the 200–350 GHz band (STAR, 2001). SOPRANO was planned to focus on stratospheric chemistry with a sub-millimeter receiver observing O<sub>3</sub>, ClO, HCl, O<sub>2</sub>, BrO, HOCl, CH<sub>3</sub>Cl, H<sub>2</sub>O, N<sub>2</sub>O, HNO<sub>3</sub> in the 500–950 GHz band. PIRAMHYD is planned to measure OH at even smaller wavelengths (2.5 and 3.5 THz) than SOPRANO (Bühler *et al.*, 1996). These instruments are planned to operate in the millimeter and sub-millimeter spectral range, allowing the retrieval of atmospheric mixing ratio profiles of several molecular species (STAR, 2001).

### 2.5.3.13 *Infrared Atmospheric Sounding Interferometer (IASI)*

The Infrared Atmospheric Sounding Interferometer (IASI) is probably the most advanced instrument carried on the MetOp satellite. The sophisticated IASI instrument is a Fourier Transform Spectrometer based on a Michelson Interferometer coupled to an integrated imaging system that observes and measures infrared radiation emitted from the Earth (Figure 2.11).

The optical interferometry process offers fine spectral samplings of the atmosphere in the infrared band between the wavelengths of 3.4 and 15.5  $\mu\text{m}$ . This enables the instrument to establish temperature and water vapor profiles in the troposphere and the lower stratosphere, as well as measure quantities of O<sub>3</sub>, CO, CH<sub>4</sub>, SO<sub>2</sub>, and other compounds (Clarisse *et al.*, 2008). The IASI system aims at observing and measuring the infrared spectrum emitted by the Earth. One of its missions is to provide information on the total amount of ozone with an accuracy of 5% and a horizontal sampling of typically 25 km. It may also provide information on ozone vertical distribution with an accuracy of 10% and a vertical resolution that provides two or three pieces of independent information.

The Infrared Atmospheric Sounding Interferometer (IASI) scanning mirror directs emitted infrared radiation from one swath into the uncovered interferometer (Figure 2.12). One swath covers 30 scan positions towards the Earth and two calibration views. One calibration view is into deep space and the other is via an internal blackbody. Each scan starts on the left with respect to the flight direction of the satellite.

The sequence concludes with the interferometer (housed in the MetOp satellite) showing incident radiation being directed through the long split opening to make



**Figure 2.11.** The MetOp satellite carrying the IASI instrument (European Space Agency).

observations through the atmosphere, the calibration process then quickly takes place. The first flight model of IASI was launched on October 15, 2006 on board the first European meteorological polar-orbiting satellites, MetOp-1. IASI delivers temperature, moisture, and ozone profile information for the upper atmosphere.

#### ***2.5.3.14 Stratospheric Wind Interferometer for Transport Studies (SWIFT)***

The Stratospheric Wind Interferometer for Transport Studies (SWIFT) is an instrument carried on the Japanese GCOM-A1 satellite designed to measure wind profiles in the stratosphere and simultaneously provide profiles of ozone density. Ozone concentration and distribution is not only based on chemical reactions but is also greatly affected by the movement of air in the stratosphere. Good knowledge of the dynamics in the stratosphere and troposphere is indispensable for the correct scientific interpretation of observed ozone distributions.

SWIFT is aimed at providing much needed information about global wind distributions in the stratosphere by measuring the thermal emission of ozone mol-

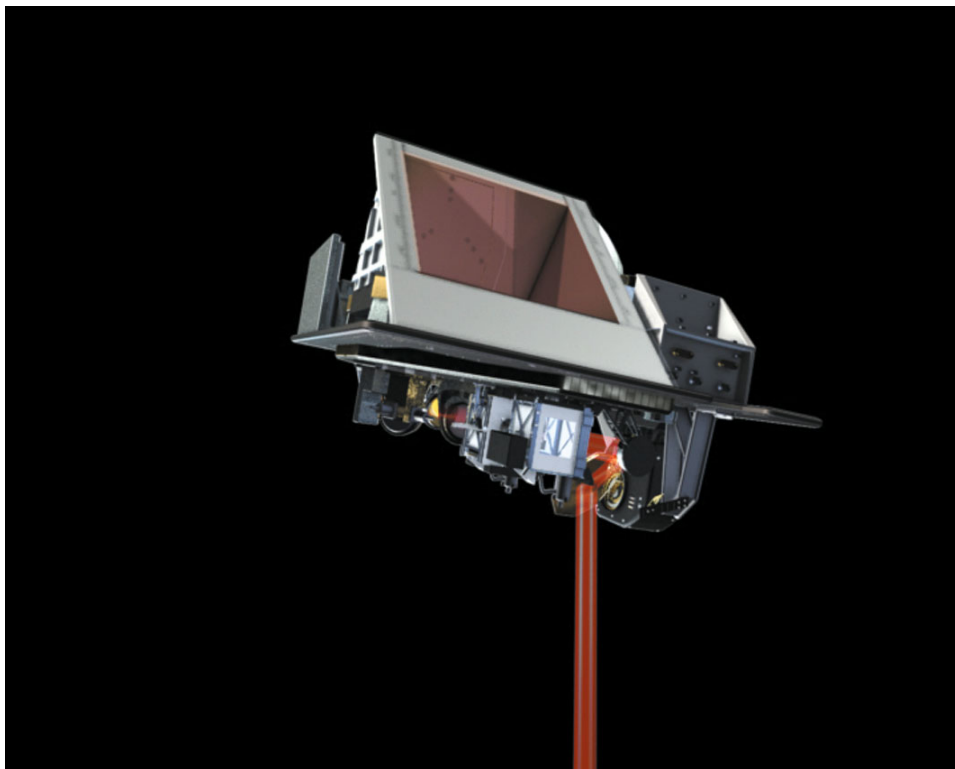


**Figure 2.12.** The scanning mirror of IASI directing emitted infrared radiation from one swath into the uncovered interferometer. One swath covers 30 scan positions towards the Earth and two calibration views. One calibration view is into deep space and the other is via an internal blackbody. Each scan starts on the left with respect to the flight direction of the satellite (*source*: European Space Agency).

ecules in the infrared at a wavelength of  $9\text{ }\mu\text{m}$ . Because ozone molecules are moving in the atmosphere by the wind, the wavelength of their emission line appears to be shifted by the Doppler effect. SWIFT is able to measure this tiny wavelength shift and, consequently, stratospheric wind can be calculated to an accuracy of  $5\text{ m s}^{-1}$ . Although this concept has already been successfully employed for wind measurements in the mesosphere with the Canadian WIND II instrument (WIND Imaging Interferometer) on the UARS satellite, this is the first time that this technique will have been used to take direct stratospheric wind measurements from space. WIND II measures winds in the upper mesosphere and lower thermosphere using Doppler shifts in visible airglow features.

Since SWIFT will observe an ozone emission line, it will also be able to measure ozone concentration simultaneously with the wind and, as such, will offer further possibilities for ozone transport studies.



### 2.5.3.15 *Sounding of the Atmosphere using Broadband Emission Radiometry (SABER)*

The Sounding of the Atmosphere using Broadband Emission Radiometry (SABER) instrument is one of four instruments mounted on the Thermosphere Ionosphere Mesosphere Energetics and Dynamics (TIMED) satellite. SABER sounds the MLTI (the mesosphere and lower thermosphere/ionosphere, 60–180 km altitude) region of the Earth's atmosphere by measuring infrared limb emission. The instrument measures accurate ground-processed values of atmospheric limb radiance to retrieve temperature, ozone, water vapor, carbon dioxide, and key parameters describing the energetic procedures of the high atmosphere. SABER results are being used to study the chemistry and dynamics of the mesosphere and the effects on the atmosphere due to major solar storm events (Cooper, 2004).

SABER (launched in 2001 and expected to be out of service by 2020) is an infrared radiometer which observes emission from the Earth's limb in 10 relatively narrow spectral intervals. It has a 2 km instantaneous field of view which scans the Earth limb from the Earth's surface to 400 km tangent altitude. Profiles of emitted radiance are recorded simultaneously through one telescope in all 10 spectral channels. These profiles are being analyzed using a variety of models in order to derive the profiles of kinetic temperature, minor species concentration, energy loss rates, solar heating rates, chemical heating rates, and radiative cooling rates. The SABER radiometer will be accurately calibrated to better than 5% (3% is the goal) in all spectral channels.

Daytime ozone is being determined by SABER by means of two different techniques. Emission by the fundamental asymmetric stretch bands of ozone in the vicinity of 9.6  $\mu\text{m}$  will be observed in order to derive the ozone concentration using emission directly from the ozone molecule itself. The SABER spectral band-pass for this channel is 1,010–1,140  $\text{cm}^{-1}$  and has been chosen to minimize the contribution from the hot bands of ozone and also from the laser bands of carbon dioxide which provided a considerable signal to the Limb Infrared Monitor of the Stratosphere (LIMS) experiment. Daytime ozone will also be inferred from measurements of the emissions from molecular oxygen dayglow at 1.27  $\mu\text{m}$ . This technique was applied in the SME experiment and will provide a second measure of daytime ozone on the SABER experiment.

Nighttime ozone concentrations will be provided by measurements at 9.6  $\mu\text{m}$ . The SABER instrument has sufficient sensitivity to record ozone emissions up to 100 km altitude (day and night). The choice of the spectral interval and the specifics of the non-LTE problem make the retrieval of nighttime ozone under non-LTE conditions relatively straightforward (Mlynchak, 1997).

### 2.5.3.16 *Superconducting Submillimeter-Wave Limb-Emission Sounder, SMILES*

The Superconducting Submillimeter-Wave Limb-Emission Sounder (SMILES) was successfully launched and attached to the Japanese Experiment Module (JEM) on the International Space Station (ISS) on September 25, 2009 (Kikuchi *et al.*, 2010). It has been making atmospheric observations since October 12, 2009 with the aid of a



4 K mechanical cooler and superconducting mixers for sub-millimeter limb emission sounding in the frequency bands of 624.32–626.32 GHz and 649.12–650.32 GHz. On the basis of the observed spectra, data processing has been retrieving vertical profiles for atmospheric minor constituents in the middle atmosphere, such as O<sub>3</sub> (with isotopes), HCl, ClO, HO<sub>2</sub>, BrO, and HNO<sub>3</sub>. Results from SMILES have demonstrated its high potential to observe atmospheric minor constituents in the middle atmosphere. Unfortunately, SMILES observations have been suspended since April 21, 2010 owing to the failure of a critical component (Kikuchi *et al.*, 2010). Previous versions of the instrument (BSMILES) were flown on balloons in 2003, 2004, and 2006.

#### 2.5.3.17 *Odin satellite*

Odin is a small Swedish satellite built jointly by Canada, France, and Finland; it was launched on February 20, 2001 to a Sun-synchronous 600 km orbit. It has two instruments, a sub-millimeter radiometer using microwave wavelengths to measure ozone, chlorine monoxide, water vapor, and other constituents, and an optical spectrograph and infrared-imaging system (OSIRIS) using UV–visible and near-infrared wavelengths for studying O<sub>3</sub>, NO<sub>2</sub>, aerosols, and other constituents. The SMR is a limb-sounding instrument that employs four tunable heterodyne receivers in the range 486–581 GHz and a 1 mm wave receiver at 119 GHz, to observe atmospheric thermal emission spectra for determination of the vertical distribution of trace species relevant to stratospheric and mesospheric chemistry and dynamics (Frisk *et al.*, 2003; Murtagh *et al.*, 2002).

Odin was the first satellite to employ sub-millimeter (480–580 GHz) radiometry of atmospheric thermal emission in a limb-sounding mode to measure the global distributions of several species important for ozone chemistry in the stratosphere (O<sub>3</sub>, ClO, N<sub>2</sub>O, and HNO<sub>3</sub>). These observations were performed simultaneously, while another mode is focused on odd hydrogen chemistry, giving H<sub>2</sub>O, O<sub>3</sub>, HO<sub>2</sub>, and CO. The retrieval method is the Optimal Estimation Method (von Scheele, 1997).

#### 2.5.3.18 *Neural Network Ozone Profile Retrieval (NNORSY)*

A variety of national and international-funded projects enabled the Center for Solar Energy and Hydrogen Research (ZSW) in Stuttgart, Germany (<http://nnorsy.zsw-bw.de/NNORSY-Intro.htm>) to develop the Neural Network Ozone Profile Retrieval (NNORSY) to provide very fast total ozone and ozone profile retrieval from different satellite instruments. NNORSY uses neural networks that are trained on GOME UV/VIS spectra by using collocated ozone profiles. These measured data include data from ozonesondes (e.g., SHADOZ, WOUDC) and from satellites (e.g., SAGE, HALOE, POAM, NOAA). The full database is divided into the training dataset and a smaller test dataset that is not used as input information for the neural nets. The whole training process was carried out in a huge number of training steps called “epochs”, and training progress could be monitored by comparing neural network outputs with the independent test dataset. Once trained, NNORSY was ready for

operational use. Since NNORSY is able to deal with instrument degradation, it can be used for near-real time applications even when the training database is slightly outdated.

#### 2.5.4 Summary of ozone-monitoring satellites

Table 2.7 explains the acronyms used for ozone-monitoring instruments found on ozone-monitoring satellites and Table 2.8 gives a chronological summary of ozone-monitoring satellites (or Space Shuttle missions).

### 2.6 OBSERVED VARIABILITY IN VERTICAL OZONE DISTRIBUTION

In the troposphere, the ozone concentration falls (on average) with increasing altitude until the tropopause is reached. In the stratosphere, ozone concentration increases rapidly with altitude to a maximum near 5 hPa, with an often appearing secondary maximum in the lower stratosphere near 100 hPa. A long-term decrease in stratospheric ozone has occurred at mid-latitudes in both hemispheres. In the Northern Hemisphere the decrease is larger in winter and spring (11% since 1979) than in summer or autumn (4% since 1979). The most dramatic changes have been seen at high latitudes in wintertime vortices over the Arctic and Antarctic. Analyses of measurements of ozone in the 1994/1995, 1995/1996, and 1996/1997 winters have shown chemical losses of up to 50% at some altitudes in each winter. Current ozone datasets came from various ozone-measuring platforms using different techniques with different spatiotemporal coverage. WMO (1999) provided the most reliable datasets with time records longer than 5 to 10 years (Table 2.9).

The Arctic vortex has been colder than usual in recent winters with record low temperatures observed during the three winters leading up to the 1997/1998 winter. It should be noted that no major mid-winter warming of the stratosphere has occurred since 1990/1991. Prior to that time, they had occurred every couple of years, and the longest gap in the 40-year record had been 4 years. Under cold conditions (temperatures below approximately 195 K or  $-78^{\circ}\text{C}$ ), polar stratospheric clouds (PSCs) can form.

Chemical reactions on PSC particles convert chlorine compounds into forms that can rapidly destroy ozone in the presence of sunlight.

It is worth noting that nacreous (mother of pearl) clouds are a rare form of stratospheric cloud which occur high up in the stratosphere. These kinds of clouds appeared, for instance, on November 30, 1999 and were widely seen across Scotland and the far north of England (Figure 2.13). They require unusually cold conditions of about  $-80^{\circ}\text{C}$  in the stratosphere to form and are usually associated with a strong northwesterly airflow over the U.K. The spectacular colors are caused by diffraction effects in particles which are very uniform and have sizes comparable with the wavelength of light. As mentioned above these clouds also provide a platform for the chemical reactions that deplete ozone, and the ozone layer crippled shortly after the November display before recovering to normal levels again. There was briefly an

**Table 2.7.** Explanation of acronyms for ozone-monitoring instruments found on ozone-monitoring satellites (Colorado State University, <http://rammb.cira.colostate.edu/dev/hilger/satellites.htm>).

<i>Instrument acronym</i>	<i>Instrument name</i>	<i>Satellite(s) or Space Shuttle mission(s)</i>
ACE-FTS	Atmospheric Chemistry Experiment-Fourier Transform Spectrometer	SciSat
ATLAS	ATmospheric Laboratory for Applications and Science	STS-45, STS-56, STS-66 (3 missions)
BUV	Backscatter UltraViolet spectrometer (and photometer)	OV1-1, OV1-10, Kosmos-45, -65, -92, -122, Nimbus-4, Explorer-55
CLAES	Cryogenic Limb Array Etalon Spectrometer	UARS
GAS	Get Away Special (canister)	STS-34, STS-41, STS-43, STS-45, STS-56, STS-62, STS-66, STS-72 (8 missions)
GOME	Global Ozone Monitoring Experiment	ERS-2, MetOp-2 (MetOp-A), MetOp-B, MetOp-C
GOMOS	Global Ozone Monitoring by Occultation of Stars	Envisat
HALOE	HALogen Occultation Experiment	UARS
HH	Hitch Hiker (payload)	STS-87, STS-107 (2 missions)
HIRDLS	High Resolution Dynamics Limb Sounder	EOS-Aura
HIRS/2	High-resolution Infrared Radiation Sounder/2	NOAA-6-NOAA-14 (9 satellites)
HIRS/3	High-resolution Infrared Radiation Sounder/3	NOAA-15-NOAA-18 (4 satellites)
HIRS/4	High-resolution Infrared Radiation Sounder/4	NOAA-19, MetOp-2 (MetOp-A), MetOp-B, MetOp-C
ILAS-1	Improved Limb Atmospheric Sounder-1	ADEOS-1
ILAS-2	Improved Limb Atmospheric Sounder-2	ADEOS-2

(continued)

**Table 2.7 (cont.).** Explanation of acronyms for ozone-monitoring instruments found on ozone-monitoring satellites (*source*: Colorado State University, <http://rammb.cira.colostate.edu/dev/hillger/satellites.htm>).

<i>Instrument acronym</i>	<i>Instrument name</i>	<i>Satellite(s) or Space Shuttle mission(s)</i>
IRFS-1	InfraRed (sounder)-1	Meteor-M1
IRFS-2	InfraRed (sounder)-2	Meteor-M2
IRIS	InfraRed Interferometer Spectrometer	Nimbus-3, Nimbus-4
IRS	InfraRed Sounder	MTG-I, MTG-S
ISAMS	Improved Stratospheric and Mesospheric Sounder	UARS
LIMS	Limb Infrared Monitor of the Stratosphere	Nimbus-7
LORE	Limb Ozone Retrieval Experiment	STS-87, STS-107 (2 missions)
LRIR	Limb Radiance Inversion Radiometer	Nimbus-4
MLS	Microwave Limb Sounder	UARS, EOS-Aura
MTVZA	Microwave Imaging/Sounding Radiometer	Meteor-M1, Meteor-M2
OLME	Ozone Layer Monitoring Experiment	FASat-Alfa, FASat-Bravo
OM	Ozone Meter	Techsat-1a, Techsat-1b/OSCAR-32
OMI	Ozone Monitoring Instrument	EOS-Aura
OMPS	Ozone Mapping and Profiler Suite	NPP/JPSS series (formerly NPOESS series)
OOAM	Orbiting Ozone and Aerosol Measurement	STEP-4
OSIRIS	Optical Spectrometer and InfraRed Imaging System	Odin
POAM	Polar Ozone and Aerosol Measurement	SPOT-3, SPOT-4
PREMOS	PRecision Monitor for OScillation measurement	Picard

SAGE	Stratospheric Aerosol and Gas Experiment	Explorer-60, ERBS, Meteor-3M-1
SBUS	Solar Backscattering UV Sounder	FY-3A, FY-3B, FY-3C
SBUV	Solar Backscatter UltraViolet radiometer	Nimbus-7
SBUV/2	Solar Backscatter UltraViolet radiometer/2	NOAA-9, NOAA-11, NOAA-13, NOAA-14, NOAA-16, NOAA-17, -18, -19
SMR	Sub-Millimeter Radiometer	Odin
SOLSE	Shuttle Ozone Limb Sounding Experiment	STS-87, STS-107 (2 missions)
SOLSTICE	SOLar STellar (Inter-)Comparison Experiment	UARS, SORCE
SSBUV	Shuttle Solar Backscatter UltraViolet radiometer	STS-34, STS-41, STS-43, STS-45, STS-56, STS-62, STS-66, STS-72 (8 missions)
SSH	Special Sensor H	DMSP-5D1-F1-DMSP-5D1-F5 (5 satellites)
SUSIM	Solar Ultraviolet Spectral Irradiance Monitor	UARS
TANSO-FTS	Thermal And Near ir Sensor for climate Observation-Fourier Transform interferometer Spectrometer	GOSAT
TES	Tropospheric Emission Spectrometer	EOS-Aura
TOM	Total Ozone Mapper	FY-3A, FY-3B, FY-3C
TOMS	Total Ozone Mapping Spectrometer	Nimbus-7, Meteor-3-5, TOMS-EP, ADEOS-1, QuikTOMS
TOU	Total Ozone Unit	FY-3A, FY-3B, FY-3C
UV	UltraViolet (radiometer, or telescope/spectrophotometer)	SAMOS-9, OAO-2, OAO-3, Explorer-64
UVISI	UV and Visible Imagers and Spectrographic Imagers	MSX
UVN	UltraViolet Visible and Near-IR sounder	MTG-S

**Table 2.8.** Chronological summary of ozone-monitoring satellites (or Space Shuttle missions) (Colorado State University, <http://rammb.cira.colostate.edu/dev/hilger/satellites.htm>).

<i>Launch date</i>	<i>Satellite (or Space Shuttle mission)</i>	<i>Instrument acronym(s) or name(s)</i>
12-08-1960	Echo-1	Ground-based analysis of sunlight reflected by the balloon (passive method, inaccurate results; solar occultation; sunlight from limb was reflected to ground from the balloon)
18-07-1962	SAMOS-9	UV radiometer (first experiment with active sensor; solar occultation limb scanning)
27-03-1964	Ariel-2	Broadband filter photometer, simple prism spectrometer (solar occultation limb scanning)
13-09-1964	Kosmos-45 (experimental weather satellite)	BUV radiometer (first known BUV or backscatter UV instrument; downward looking)
21-01-1965	OV1-1	BUV radiometer (downward looking, 30° left of nadir)
17-04-1965	Kosmos-65 (experimental weather satellite)	BUV radiometer
16-10-1965	Kosmos-92 (experimental weather satellite)	BUV radiometer
25-06-1966	Kosmos-122 (pre-Meteor weather satellite)	BUV radiometer
11-12-1966	OV1-10	BUV spectrophotometer
28-07-1967	OGO-4	Ebert–Fastie scanning spectrometer
07-12-1968	OA0-2	UV telescope/spectrophotometer (starlight occultation limb scanning)
13-04-1969	Nimbus-3	IRIS
08-04-1970	Nimbus-4	BUV spectrometer, IRIS

21-08-1972	OA0-3	UV telescope/spectrometer (starlight occultation limb scanning)
12-06-1975	Nimbus-6	LRIR (limb scanning)
20-11-1975	Explorer-55 (AE-5 or AE-E)	BUV (solar occultation limb scanning rather than downward looking)
11-09-1976	DMSP-5D1-F1	SSH (multichannel filter radiometer)
04-06-1977	DMSP-5D1-F2	SSH (multichannel filter radiometer)
01-05-1978	DMSP-5D1-F3	SSH (multichannel filter radiometer)
24-10-1978	Nimbus-7 (longest lasting mission; data 1978-1993)	LIMS (limb scanner, an update of the LRIR), TOMS-1, SBUV
18-02-1979	Explorer-60 (AEM-B)	SAGE-1
06-06-1979	DMSP-5D1-F4	SSH (multichannel filter radiometer)
27-06-1979	NOAA-6	HIRS/2 (atmospheric sounder with 9.7 $\mu$ m ozone channel)
14-07-1980	DMSP-5D1-F5 (launch failed)	SSH (multichannel filter radiometer)
23-06-1981	NOAA-7	HIRS/2
06-10-1981	Explorer-64/SME	UV ozone experiment, Four-Channel Infrared Radiometer, Airglow Instrument
28-03-1983	NOAA-8	HIRS/2
05-10-1984	ERBS (launched from STS-41G)	SAGE-2
12-12-1984	NOAA-9	SBUV/2 (based on the SBUV/TOMS-1 flown on Nimbus-7), HIRS/2
17-09-1986	NOAA-10	HIRS/2

(continued)



**Table 2.8** (cont.). Chronological summary of ozone-monitoring satellites (or Space Shuttle missions) (*source*: Colorado State University, <http://rammb.cira.colostate.edu/dev/hillger/satellites.htm>).

<i>Launch date</i>	<i>Satellite (or Space Shuttle mission)</i>	<i>Instrument acronym(s) or name(s)</i>
24-09-1988	NOAA-11	SBUV/2, HIRS/2
18-10-1989	STS-34	SSBUV-1 (GAS canister)
06-10-1990	STS-41	SSBUV-2 (GAS canister)
14-05-1991	NOAA-12	HIRS/2
02-08-1991	STS-43	SSBUV-3 (GAS canister)
15-08-1991	Meteor-3-5 (Meteor-TOMS)	TOMS-2
12-09-1991	UARS (launched from STS-48)	CLAES, ISAMS, HALOE, SUSIM, MLS, SOLSTICE
24-03-1992	STS-45	SSBUV-4 (GAS canister, ATLAS-1 payload)
08-04-1993	STS-56	SSBUV-5 (GAS canister, ATLAS-2 payload)
09-08-1993	NOAA-13	SBUV/2, HIRS/2
26-09-1993	SPOT-3	POAM-2 (solar occultation limb scanning)
03-04-1994	STS-62	SSBUV-6 (GAS canister)
03-11-1994	STS-66	SSBUV-7 (GAS canister, ATLAS-3 payload)
30-12-1994	NOAA-14	SBUV/2, HIRS/2
20-04-1995	ERS-2	GOME-1 (BUV technique)

28-03-1995	TechSat-1a microsatellite (failed)	OM-2 UV radiometer (SBUV technique)
31-08-1995	FASat-Alfa microsatellite (failed to separate from Sich-1)	OLME
11-01-1996	STS-72	SSBUV-8 (GAS canister)
24-04-1996	MSX	UVISI
02-07-1996	TOMS-EP	TOMS(-3)
17-08-1996	ADEOS-1	TOMS(-4), ILAS-1
23-10-1997	STEP-4	OOAM
13-11-1997	STS-87	SOLSE-1 (HH payload), LORE-1
24-03-1998	SPOT-4	POAM-3 (solar occultation limb scanning)
13-05-1998	NOAA-15	HIRS/3
10-07-1998	FASat-Bravo microsatellite	OLME
1999	Meteor-3M-2 (this Meteor-3M-1 follow-up was canceled in 1999)	SAGE-3
10-07-1998	TechSat-1b/OSCAR-32 microsatellite	OM-2 UV radiometer (SBUV technique)
21-09-2000	NOAA-16	SBUV/2, HIRS/3
20-02-2001	Odin	OSIRIS, SMR
21-09-2001	QuikTOMS (launch failed)	TOMS-5

(continued)

**Table 2.8** (cont.). Chronological summary of ozone-monitoring satellites (or Space Shuttle missions) (*source*: Colorado State University, <http://rammb.cira.colostate.edu/dev/hillger/satellites.htm>).

<i>Launch date</i>	<i>Satellite (or Space Shuttle mission)</i>	<i>Instrument acronym(s) or name(s)</i>
10-12-2001	Meteor-3M-1	SAGE-3
01-03-2002	Envisat	GOMOS (starlight occultation limb scanning)
24-06-2002	NOAA-17	SBUV/2, HIRS/3
14-12-2002	ADEOS-2	ILAS-2
16-01-2003	STS-107 (lost on entry)	SOLSE-2 (HH payload), LORE-2 (limb-viewing spectrometers)
25-01-2003	SORCE	SOLSTICE
13-08-2003	SciSat	ACE-FTS
15-07-2004	EOS-Aura (formerly EOS-Chem)	OMI, HIRDLS, TES, MLS (OMI-SBUV technique; data similar to earlier TOMS data, but higher horizontal resolution; HIRDLS and MLS limb scanners; TES limb and nadir scanner)
20-05-2005	NOAA-18	SBUV/2, HIRS/4
19-10-2006	MetOp-2 (MetOp-A)	GOME-2, HIRS/4
27-05-2008	FY-3A	TOM or TOU, and SBUS
06-02-2009	GOSAT (formerly GCOM-A1)	TANSO-FTS (similar to SciSat's ACE-FTS), ODUS (Ozone Dynamics UV Spectrometer), a SBUV instrument, was planned but not used
06-02-2009	NOAA-19	SBUV/2, HIRS/4

17-09-2009	Meteor-M1 (or Meteor-M) (replacement for Meteor-3M)	MTVZA imager/sounder; IRFS-1
15-06-2010	Picard	PREMOS
04-11-2010	FY-3B	TOM or TOU, and SBUS
Future satellites with ozone equipment		
201?	FY-3C	TOM or TOU, and SBUS
201?	Meteor-M2	MTVZA imager/sounder; IRFS-2 advanced IR sounder
201?	CX-1 microsatellite (University of Colorado)	(BUV?) spectrophotometer
201?	DSCOVR (formerly Triana, or “Gore Sat”) (to rest at Lagrange point)	BUV?
201?	NPP/JPSS series (formerly NPOESS series)	OMPS (nadir-viewing UV sensor and limb-viewing UV/visible sensor)
2012?	MetOp-B	GOME-2, HIRS/4
2016?	MetOp-C	GOME-2, HIRS/4
2016–2030	MTG-I	IRS
2018–2026	MTG-S	IRS, UVN

**Table 2.9.** Inventory of the most “reliable” datasets with time records longer than 5 years of OVP (Ozone Vertical Profile) (WMO, 1999).

<i>Platform</i> <i>Satellites</i>	<i>Middle/Upper stratosphere (Z &gt; 25 km)</i>	<i>Low stratosphere (Z &lt; 25 km)</i>	<i>Troposphere</i>
SAGE I	Feb. 1979—Nov. 1981	Feb. 1979–Nov. 1981	
SAGE II	Oct. 1984—present	Oct. 1984–present	
SBUV + SBUV/2	1978–present		
HALOE	Oct. 1991–present	Oct. 1991–present	
MLS	Oct. 1991–present	Oct. 1991–present	
Ground-based microwave	1989–present	1989–present	
Umkehr/Dobson	1957–present		
Lidar	1990–present	1985–present	1990–present
Balloonborne sondes		1965–present	1965–present

**Figure 2.13.** Cloud detail view from an image taken in Aberdeen (Scotland) with a digital camera (© George Soja and Brian Ward, Aberdeen).

ozone hole over Europe arising from the accelerated ozone-depleting reactions that occur on cloud particles. There was another display of nacreous clouds on January 29, 2000 which was visible from the south of England (<http://www.nezumi.demon.co.uk/astro/nacreous/3/nacreous3.htm>).

In general the Arctic experiences highly extreme cold as well as sudden stratospheric warmings (SSWs) at times. As a result the degree of ozone loss is mostly controlled by the strength of the vortex and magnitude of air temperature

within. For instance, according to Kuttippurath *et al.* (2010a, b) the winters 1995, 1996, 2000, and 2005 were very cold and cumulative total ozone loss was as high as  $\sim 25\text{--}35\%$  (WMO, 2007). On the other hand, the winters 1997–1999, 2001, 2002, 2006, and 2009 were relatively warm and the loss was minimal about 10–15%, while the winters 2003, 2007, and 2008 were moderately cold and, hence, the loss was on an average scale of about 15–20% (Goutail *et al.*, 2010; WMO, 2007).

As far as the upper atmosphere is concerned the temperature shows an annual variation in the upper mesosphere above about 65 km with the largest values in winter, but this general behavior is interrupted by SSW events resulting in a cooling of the upper-mesosphere/mesopause region (Sonnemann *et al.*, 2007). The chemical reaction rates are temperature dependant and entail an ozone decrease if the temperature increases. This should reduce the wintertime enhancement of ozone, but to a different degree between daytime and nighttime ozone. However, the effect is insignificant close to the turning point of annual temperature variation at 65 km where the annual variation of temperature is very small. The influence of SSWs on the chemistry was investigated by Sonnemann *et al.* (2006). They found that an SSW is able to modulate ozone concentrations. During major SSWs the west wind changes into a summery east wind system, prolonging the time of sunset and reducing the nighttime ozone level. However, the decrease in temperature has the tendency to enhance the ozone level so that the resulting effect is damped or even reversed. As the zonal wind during daytime does not strongly affect ozone, the ozone increases during daytime when the temperature decreases.

Sonnemann *et al.* (2007) also suggested that at sunset the wintry west wind system conveys an air parcel more quickly through this period and shortens the time of effective odd oxygen destruction by catalytic cycles. This effect results from the imbalance between net odd oxygen production by the dissociation of molecular oxygen and the ozone dissociation rate transforming only one odd oxygen constituent into another. Atomic oxygen is then involved in the odd oxygen-destroying catalytic cycle.

We shall now briefly discuss some outstanding field campaigns.

### 2.6.1 EASOE

A major European campaign, the European Arctic Stratospheric Ozone Experiment (EASOE) (Section 6.6.3.1) was organized to study the polar regions during the winter of 1991/1992. Particular goals were:

- to measure the change in ozone concentration with altitude throughout the winter;
- to measure the concentrations of other trace chemical species (especially chlorine and nitrogen);
- to investigate the role of polar stratospheric clouds, and in particular to study dehydration and denitrification of the Arctic stratosphere;
- to study the meteorological processes that move chemically perturbed air southward.



Measurements were made using ground-based instruments at 16 sites ranging from the Arctic Circle to southern Europe from large stratospheric balloons and from three research aircraft. Forty-three stratospheric balloons, capable of carrying scientific payloads of up to 500 kg directly into the ozone layer, were launched from the Swedish Space Corporation rocket range at ESRANGE (European Space Range) near Kiruna, Sweden. In addition, over 1,000 ozonesondes were launched on small balloons from more than 20 sites. A wide variety of meteorological information was provided by the various European meteorological services, including some information provided especially for EASOE scientists.

Much new information was gained. Despite this activity, many intriguing questions remain: What causes the mid-latitude loss? How are the losses over the poles linked to those at mid-latitudes? (see Chapters 3 and 4).

### 2.6.2 SESAME

In 1994 and 1995 European scientists conducted SESAME, the Second European Stratospheric Arctic and Mid-latitude Experiment, to investigate the processes occurring at both high and mid-latitudes and to see how they are linked (see Section 6.6.3.1). At the same time a U.S.-led expedition was looking at similar processes in the Southern Hemisphere.

### 2.6.3 THESEO

The Third European Stratospheric Experiment on Ozone (THESEO) was organized to investigate long-term ozone loss over northern high and mid-latitudes during 1998 and 2000. The processes involved include both those that occur over mid-latitudes and those resulting from the exchange of air between the mid-latitude stratosphere and neighboring parts of the atmosphere. In the first few months field measurements were made mainly at mid and high latitudes and focused on a limited number of specific processes. From the end of November until the beginning of February (1997/1998) the temperature within the vortex fell below the critical temperature for the formation of polar stratospheric clouds (PSCs). However, because of the occurrence of a series of mid-stratospheric warmings the extent of the PSCs was not large. Moreover, outside the vortex in the upper stratosphere unusually high temperatures were observed. This winter was finally warmer than the previous three (exceptionally cold) winters and, therefore, TOC values were higher than those in the past few winters. These higher TOC values masked any chemical ozone loss (estimated to be 15–20% inside the vortex).

### 2.6.4 SOLVE

The SOLVE campaign was designed to examine the processes that control polar to mid-latitude stratospheric ozone levels. The mission was conducted during the 1999–2000 northern winter from Kiruna (Sweden). The SOLVE campaign employed NASA ER-2, NASA DC-8, and OMS *in situ* and remote-sensing balloon payloads,

ground station observations, and an extensive theory team. The mission also acquired correlative measurements needed to validate the Stratospheric Aerosol and Gas Experiment (SAGE) III satellite mission and used these satellite measurements to help quantitatively assess high-latitude ozone loss. The results of SOLVE both expanded our understanding of polar ozone processes and provided greater confidence in our current ozone-monitoring capabilities. This knowledge provides the basis for setting sound public policies which will help to preserve the Earth's ozone layer.

During the 1999/2000 winter, the THESEO 2000 campaign sponsored by the European Union (consisting of a core of 12 major EU-funded projects) and the NASA-sponsored SAGE III SOLVE campaign obtained measurements of ozone and other atmospheric gases and particles using satellites and aircraft; large, small, and long-duration balloons; and ground-based instruments. Scientists from Europe, the United States, Canada, Russia, and Japan joined forces in mounting the biggest field measurement campaign yet to measure ozone amounts and changes in the Arctic stratosphere. The total amount of information collected by the THESEO 2000/SOLVE campaign was more extensive than any information collected by past polar measurement campaigns. Most of the measurements were made near Kiruna, Sweden, with additional measurements being taken from satellites and through a network of stations at mid and high northern latitudes.

### 2.6.5 ORACLE-O<sub>3</sub>

The acronym comes from the title "Ozone layer and uv RADIation in a changing CLimate Evaluated during the International Polar Year (IPY).

The IPY themes that were addressed are as follows:

1. Current state of the environment
2. Change in the polar regions
3. Polar-global linkages/tele-connections
4. Exploring new frontiers
5. The polar regions as vantage points
6. The human dimension in polar regions.

The project was divided into seven main activities: (1) ozone loss (detection and impact on UV radiation); (2) PSCs (polar stratospheric clouds) and cirrus; (3) atmospheric chemistry; (4) UV radiation; (5) ozone, climate change, and feedback; (6) data management; and (7) education, outreach, and communication. The project implied precise quantification of polar ozone losses in both hemispheres achieved with concerted international campaigns during which hundreds of ozone-sondes were launched in real time coordination from station networks in the Arctic and Antarctic. Satellite coverage of ozone and ozone-depleting substances were made from satellites such as ENVISAT, Aura, ACE, Odin, POAM III, and SAGE III along with ground-based station data.

### 2.6.6 SCOUT-O3

SCOUT-O3 was a European Commission Integrated Project with €15 million of funding. The project had 59 partner institutions and over 100 scientists involved from 19 countries. The project commenced on May 1, 2004 and ran until April 31, 2009.

SCOUT-O3's aim was to provide predictions about the evolution of the coupled chemistry/climate system, with emphasis on ozone change in the lower stratosphere and the associated UV and climate impact, to provide vital information for society and policy use.

SCOUT-O3 was structured to investigate eight scientific activities, as follows:

- ozone, climate, and UV predictions
- SCOUT-O3 tropical
- extratropical ozone and water vapor
- UV radiation
- chemistry and particles: studies of kinetics, photochemistry, heterogeneous processes, and nucleation
- global diagnostic chemical transport modeling
- SCOUT-O3 database and public outreach
- management.

### 2.6.7 Match

The Match campaigns are part of the ORACLE-O<sub>3</sub> project (see Section 2.6.5) within the International Polar Year (IPY), which actually covers two years—March 2007 to March 2009 (see also Section 6.6.3.1).

The two main aims of the Match campaigns are:

1. to measure chemical ozone loss in polar regions; and
2. to check our understanding of the underlying processes.

As mentioned above, during the North Hemisphere winter 1991/1992 a concerted campaign funded by the EU and national agencies (EASOE) took place. The activities included the launch of a large number (~1,400) of ozonesondes in the Arctic and in the mid-latitudes. This dataset was used afterwards to determine Arctic ozone losses for the first time with the Match Method. Since the launches were not coordinated only those matches that happened by chance were used. Fortunately, because of the large number of soundings enough matches were found for a successful analysis. It was in this way that the method was established and for the Second European Stratospheric Arctic and Mid-latitude Experiment (SESAME) in the winter 1994/1995 the method was advanced to its active form with coordinated launches as described above. In nearly every Arctic winter since then a Match Campaign has been carried out. The only exceptions were the winters 2001/2002 and 2003/2004, which were relatively warm stratospheric winters with minor ozone

losses. In the meantime, the winters 1992/1993 and 1993/1994 were analyzed by the passive Match approach, too. In total, analyzed ozonesonde Match data exist for 12 Arctic winters and one Antarctic winter (2003).

### 2.6.8 ARC\_IONS

The Arctic Intensive Ozonesonde Network (ARC-IONS)—which covered Canada, Alaska, and the mid-upper U.S.—consisted of two field phases with 18 sites, most launching daily (square symbols in Figure 2.14) (<http://croc.gsfc.nasa.gov/arcions>).

ARC-IONS is one of the three coordinated ozonesonde networks, the IONS series, that operated over North America in support of satellite validation and multiple aircraft and ground sites during field campaigns (Figure 2.14). During IONS-04, the 250+ profiles obtained over eastern North America represented the largest single set of free tropospheric ozone measurements ever compiled for that region. In IONS-06 and ARC-IONS (2008), multiple phases (two 3 to 4-week campaigns) and a larger set of sites expanded the IONS dataset to a total of 1,400 ozone



**Figure 2.14.** Locations of IONS sites: IONS-04 (INTEX Ozonesonde Network Study), where INTEX = Intercontinental Chemical Transport Experiment, conducted in July–August 2004; IONS-06, March–May 2006, supporting INTEX-B, and August–September 2006. ARC-IONS, Arctic Intensive Ozonesonde Network, April 2008 and June–July 2008, shifted to higher latitudes (*source: Thompson et al., 2011*).

and pressure–temperature–humidity profile sets (IONS data are available at <http://woudc.org>).

IONS data are used for forecasting and flight planning during the field phase to determine ozone budgets, satellite validation, and evaluation of chemical transport models at various scales. During field phases, the ozone profiles are used in a manner similar to the Match concept.

The scientific goals of IONS-04 were to study continental outflow patterns and variability during INTEX-NA, particularly major regions of pollution flow above the boundary layer and the convective contribution to ozone in the middle to upper troposphere. IONS-04 profiles tracked pollution from Alaskan and Canadian forest fires and from New York City. In addition to the sonde coordination with aircraft and surface measurements in INTEX-A, the large number of IONS-04 profiles enabled new air quality model validation exercises. Thompson *et al.* (2011) suggested that, whereas the Canadian air quality forecast models AURAMS and CHRONOS show considerable skill at predicting ozone in the planetary boundary layer and just above (Figure 2.15), they have large errors in the free troposphere, owing largely

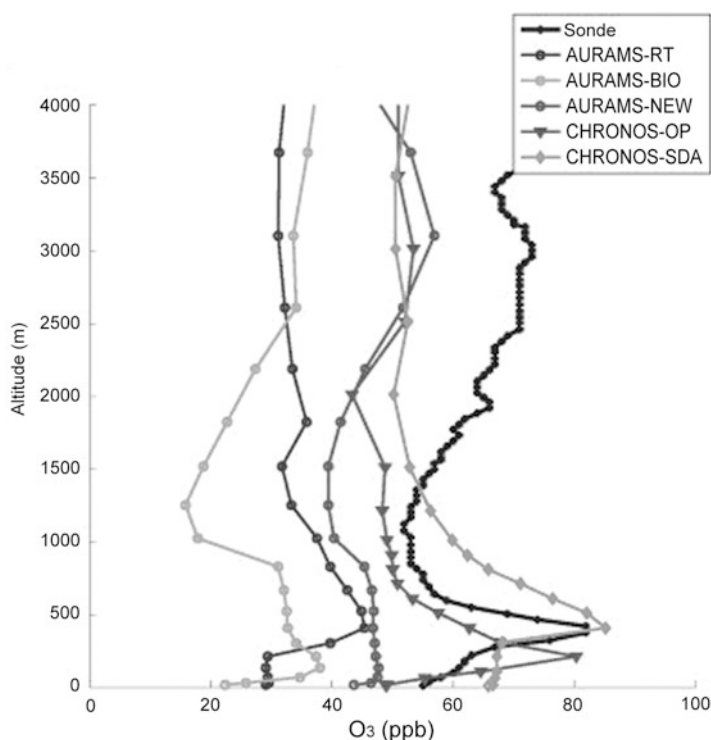


**Figure 2.15.** Comparisons of several Canadian air quality models with IONS-04 sondes (line without symbol) at the surface to 4 km. AURAMS = A Unified Regional Air Quality Modeling System; CHRONOS = Canadian Hemispheric and Regional Ozone and NO<sub>x</sub> System (Thompson *et al.*, 2011).

to the inadequate treatment of model domain boundaries (including the upper boundary).

The scientific goals of IONS-06 were: the determination of intercontinental transport, primarily the flux of ozone from Asia to and across the North American continent; the evaluation of tropospheric ozone budgets, including the stratospheric component; and the validation of Aura satellite tropospheric ozone. IONS-06 data provided surprising new insights on tropospheric processes and their effect on the ozone budget. Sub-tropical ozone over Mexico City and Houston in spring revealed robust wave activity in the free troposphere and tropopause region. In summer, although lightning and convection influences over these sites were intense, 39% of the soundings exhibited stratospheric signatures. Over the central to eastern U.S. and Canada during the summer phase of IONS-06, a similar mixture of interleaved sources in ozone profiles to those in IONS-04 was observed (Thompson *et al.*, 2011).

Remote Sensing and Atmospheric Ozone  
Human Activities versus Natural Variability

Cracknell, A.P.; Varotsos, C.A.

2012, XLI, 662 p. 183 illus., 69 illus. in color., Hardcover

ISBN: 978-3-642-10333-9